https://doi.org/10.5194/egusphere-2025-3580
Preprint. Discussion started: 8 August 2025

Hydrothermal activity indirectly influences ice nuclei particles in seawater and nascent sea spray of the Subtropical Pacific Ocean

Yannick Bras[1], Evelyn Freney[1], Mar Benavides[2,3,4], Estelle Bigeard[5], Gabriel Dulaquais[6], Céline Dimier[7], Laetitia Bouvier[1], Mickaël Ribeiro[1], Cécile Guieu[7], Sophie Bonnet[2] and Karine Sellegri[1]

[1]Université Clermont Auvergne, Observatoire du Globe de Clermont-Ferrand, CNRS, Laboratoire de Météorologie Physique (LaMP), Aubière, France

[2]Aix Marseille Université, Université de Toulon, CNRS, IRD, MIO UM 110, 13288, Marseille, France

[3]Turing Center for Living Systems, Aix-Marseille University, 13009 Marseille, France

[4]National Oceanography Centre, European Way, Southampton, SO14 3ZH, United Kingdom

[5]Station Biologique de Roscoff, Sorbonne Université, 29680 Roscoff, France

[6]Laboratoire LEMAR, Institut Universitaire Européen de la Mer, 29280 Plouzané, France

[7]Laboratoire d'Océanographie de Villefranche, Villefranche-sur-Mer, France

Correspondence to: Karine Sellegri (k.sellegri@opgc.fr); Yannick Bras (yannick.bras@protonmail.com)

Abstract. Particles of marine origin may act as ice nuclei when clouds form and therefore influence cloud properties and lifetime. Here we investigate the abundance of Ice Nuclei Particles in bulk seawater (INP_{SW}) collected in natural seawater of the Western Tropical South Pacific and in sea spray aerosol (INP_{SSA}) artificially generated from the surface seawater. The study area was separated into two oligotrophic zones (the Melanesian Basin and the Western South Pacific Gyre), and a mesotrophic one (the Lau basin), characterized by high plankton biomass due iron fertilization by underwater hydrothermal activity of the Tonga volcanic arc. Our results show that INP_{SW} were on average 80% heat labile, strongly suggesting a biological origin. INP_{SW} concentrations were two-fold higher in the Lau basin as compared to both oligotrophic areas at all freezing temperatures. This trend is consistent with a higher abundance of planktonic microorganisms, pigments and particulate organic carbon (POC) concentrations in the Lau basin. Over the whole cruise transect, medium to strong correlations were found between INP_{SW} concentrations and pigments (notably with bacteriochlorophyll-a and carotene), bacterial abundance and POC. The heat stable fraction of INP_{SW} exhibited correlations with Dissolved Organic Carbon (DOC) concentrations and were not as variable as the heat labile INP_{SW}. In the nascent sea spray, INP_{SSA} were also mostly heat labile in coherence with the INP_{SW}. INP_{SSA} were predominantly (60 %), submicron in size (presumed originating from film drops), but the supermicron INP_{SSA} constituted 40% of the INP_{SSA} and were all heat labile (presumably originating from jet drops). Supermicron INP_{SSA} were between 60 to 80% heat stable with a high variability between samples, indicating different nature of the two fractions of INPs. Supermicron INP_{SSA} were generally more abundant in the Lau basin, while submicron INP_{SSA} did not exhibit any significant difference between the three regions. We report a transfer function of seawater INPs to SSA INPs of 1.70 $m^{-2}.L_{SW}$ and 3.3 $m^{-2}.L_{SW}$ for heat stable INPs, hinting that heat stable INPs were more efficiently transferred to the SSA. Our results suggest that hydrothermal activity indirectly enhances the INP concentration of surface waters, through boosting the biological

https://doi.org/10.5194/egusphere-2025-3580
Preprint. Discussion started: 8 August 2025

activity, which results in increases of the ice forming ability of supermicron sea spray particle. Given the extent of hydrothermal activity throughout the global Ocean, its impact on cloud properties should be considered in future ocean-atmosphere interaction studies.

1 Introduction

Marine aerosols, or sea spray aerosols (SSA) are generated from breaking waves as bubbles bursting at the sea-air interface. As they rise up the water column, bubbles scavenge organic matter on their surface, which is the main mechanism for the enrichment of the surface micro-layer (SML), with biologically originating organic material (Cunliffe et al., 2013). Once bubbles burst, the organic material is ejected resulting in submicrometer film-drops that may be enriched in biological material compared to larger jet drops, more representative of bulk seawater (Aller et al., 2005; Russell et al., 2010; Schmitt-Kopplin et al., 2012). Film and jet drops residues, i.e. SSA, can be uplifted in the atmosphere (Cochran et al., 2017), where they act as cloud condensation nuclei (CCNs) and/or Ice Nuclei Particles (INPs). These particles of marine origin have thus an impact on clouds microphysical properties, phase (liquid, mixed or ice), optical and dynamical properties, and ultimately on its precipitation and therefore on cloud lifetime (Brooks and Thornton, 2018).

Previous observations have shown that the ice nucleating ability of marine particles is lower than those of terrestrial particles (DeMott et al., 2016; Porter et al., 2022; Wilbourn et al., 2024). However, due to their predominance as oceans cover more than 70% of the Earth, marine aerosols with ice nucleating (IN) properties are of primary importance. SSA can contain biogenic material that may be active at warmer temperatures (Burrows et al., 2013; Vergara-Temprado et al., 2017; Wilson et al., 2015; Gong et al., 2020; Kawana et al., 2024) and therefore initiate precipitation earlier in the cloud life cycle (Lin et al., 2022), especially at mixed-phase clouds temperatures (> −20 °C, Raatikainen et al., 2021).

An increasing number of studies have recently attempted to link ocean biogeochemistry with the IN properties of marine aerosols through ship-based (e.g. McCluskey et al., 2018c; Trueblood et al., 2021; Kawana et al., 2024), ground-based (e.g. McCluskey et al., 2018a; Porter et al., 2022; Willbourn et al., 2024) or aircraft (e.g. Knopf et al., 2022; Moore et al., 2024) measurements. Several studies have linked the IN activity of SSA or seawater samples with phytoplankton abundances, such as the cyanobacterium *Prochlorococcus* (Wolf et al., 2019), the diatom *Thalassiosira Pseudonana* (Knopf et al., 2011a; Wilson et al., 2015) or other biological indicators (Hill et al., 2023) such as chlorophyll-*a* (Kawana et al., 2024). McCluskey et al. (2018c) linked an increase in INP concentrations with plankton blooms in both open ocean and coastal sites, and heat labile material, indicative of biological components (Murray et al., 2012), was found to be the dominant type of INP in the Arctic SML (Irish et al., 2017). Several studies linked both dissolved and particulate organic matter in seawater and in the nascent

https://doi.org/10.5194/egusphere-2025-3580
Preprint. Discussion started: 8 August 2025

SSA to its INP concentration (Trueblood et al., 2021; Knopf et al., 2022; Knopf et al., 2023). Although there seems to be a clear impact of ocean biology on the variability of INPs in seawater and SSA, the nature of IN-active material and the drivers of IN properties of sea spray remains an open question, and very little is known about the drivers of IN properties of sea spray with only a few studies focused on the Mediterranean sea (Trueblood et al., 2021) and in the Southern Ocean (e.g. McCluskey et al., 2018a; Miyakawa et al., 2023; Moore et al., 2024. Even less is known on the ice nucleating properties of particles originating from hydrothermal activity. IN properties of aerosols and materials issued from volcanic processes have indeed been solely investigated in the atmosphere. Atmospheric volcanic ash has long been suggested to influence heterogeneous ice nucleation (Isono et al., 1959; Hobbs et al., 1971; Durant et al., 2008; Fornea et al., 2009; Seifert et al., 2011) and Genareau et al. (2018) showed that volcanic ash is a better ice nuclei when it has a high surface area, small average grain size, high K_2O content, and low MnO content. IN properties of seawater at the vicinity of hydrothermal sources are, to the best of our knowledge, completely unexplored.

In this study, we investigated the IN properties of the bulk seawater and the SSA in the framework of the TONGA project (shallow hydroThermal sOurces of trace elemenNts: potential impacts on biological productivity and bioloGicAl carbon pump, https://doi.org/10.17600/18000884). This project aimed at investigating the role of shallow hydrothermal activity on ocean productivity and carbon sequestration to the deep ocean. It provided a unique opportunity to study the link between surface ocean processes and the ocean-atmosphere link in the Western Tropical South Pacific (WTSP). The WTSP is characterized by contrasted ocean provinces, with oligotrophic (i.e. nutrient poor) waters in the east, separated by an area of high biological activity caused by iron fertilization from hydrothermal activity and subsequent diazotrophic plankton blooms near the Tonga-Kermadec volcanic arc (Bonnet et al., 2018; Moutin et al., 2018; Bonnet et al., 2023). Here we explore how the IN properties of seawater evolve under different exposure to the presence of hydrothermal sources, and when naturally mixed with particles of volcanic origin at the seafloor. We also investigate the impact of submarine volcanic activity and hydrothermal sources on INP concentrations of surface seawater and SSA artificially generated from this surface seawater.

2 Methods

2.1 Ship campaign and experimental procedures

The TONGA project (shallow hydroThermal sOurces of trace elemenNts: potential impacts on biological productivity and bioloGicAl carbon pump), is an interdisciplinary research project examining the role of micronutrients from hydrothermal sources on ocean productivity, carbon sequestration and impact on the atmosphere. The TONGA cruise campaign (https://doi.org/10.17600/18000884) took place on board the French R/V *L'Atalante* in the region of the Tonga volcanic arc in the WTSP. The ship departed from New Caledonia (22° 21'S, 166°59'E) on 1 November 2019, and performed two transects West-East-West with the most eastern point (20°19'S, 166°33'W) on 19 November 2019 (Fig 1). The transects cross a section of the Tonga-Kermadec volcanic arc, that stretches for 3000 km, from south of the American Samoa to New Zealand's

https://doi.org/10.5194/egusphere-2025-3580
Preprint. Discussion started: 8 August 2025

Northern Island. The transects can be separated into three main seawater types (Bonnet et al., 2018; Moutin et al., 2018; Bonnet et al., 2023). The oligotrophic Melanesian waters (MEL), east of the 180ºE; the mesotrophic, relatively nutrient-rich, Lau Basin waters (LAU, 180ºE-175ºE) which are influenced by hydrothermal sources issued from volcanism; and the ultra-oligotrophic South Pacific Gyre waters (WGY, east of the 175ºE longitude).

Measurements were performed both on the surface seawater (SSW) and on the generated SSA. SSA was generated using the same technique as described in Sellegri et al. (2005), Schwier et al. (2015) and Trueblood et al. (2021). Briefly, the underway seawater (UWAY, depth ~5 m) is continuously injected in a 10 L tank through 1 mm jets, creating bubbles in the halfway filled seawater part of the tank, in a similar way than the breaking wave process. Sea spray generated via bubble bursting is emitted into the headspace of the tank which is flushed with particle filtered air. The tank's headspace, filled with nascent sea spray particles, is continuously sampled for analysis of the sea spray size distribution, chemical composition and INP and CCN properties. Bulk SSW was collected from the UWAY with a time resolution of 4 hours during daytime, using 50 mL Falcon tubes that were immediately stored at -20 °C for later analysis at the laboratory. Several seawater samples were also collected with CTDs (Conductivity, Temperature, Depth probes) at 12 different depths, from 4.5 m to 400.9 m at fixed stations along the transect (Fig. 1). Two of the stations were in the vicinity of the Simone and Panamax submarine volcanoes, where longer measurements could be performed. As INP concentrations were only sampled from surface seawater, we only use here the results from samples taken at 4.5 m depth. CTD samples were then used to determine pigments, POC concentrations and diazotrophs and other cyanobacteria abundances as detailed in section 2.2.

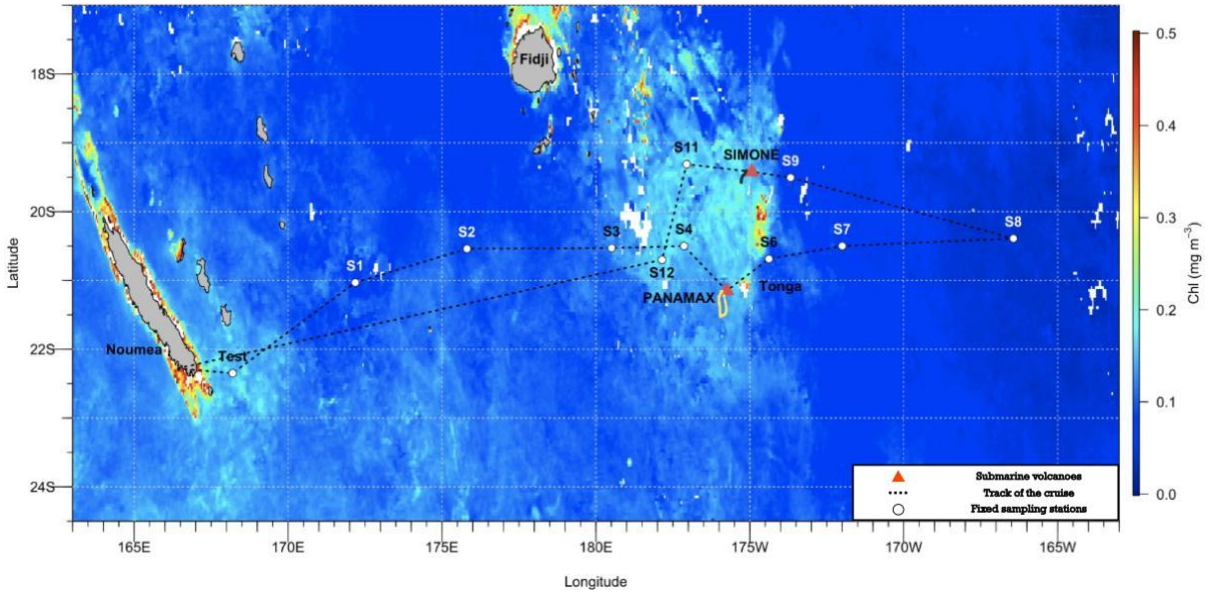

https://doi.org/10.5194/egusphere-2025-3580
Preprint. Discussion started: 8 August 2025

Figure 1 – Track of the TONGA cruise from 01/11/2019 to 01/12/2019 and surface chlorophyl-a with the location of the fixed sampling stations S1 through S12, including the Simone (Station 10) and Panamax (Station 05) submarine volcanoes. Stations S1 and S2 are in the MEL. Figure adapted from the TONGA mission report (https://doi.org/10.17600/18000884).

2.2 Seawater analytical procedures

The data obtained from the methods described in this section are available in the TONGA cruise biogeochemical dataset (Guieu et al., 2022).

Seawater properties (salinity, temperature) were measured continuously using a Thermo-salinograph (https://campagnes.flotteoceanographique.fr/campagnes/18000884/). Seawater surface tension was measured on samples taken from the ship's underway system using a dynotester instrument with a time resolution of 5 to 12 hours. Once the samples were taken, they were stored for a few hours at -20 °C, then brought back to room temperature with a surface tension measurement performed for each temperature with a resolution of about 1 °C. Flow Cytometry (FCM) analyses were performed at the Roscoff Biological station from seawater samples taken from the underway seawater system and fixed with the same time resolution as the samples taken for surface tension analysis. This allows the measurement of microorganisms such as cyanobacteria (*Prochlorococcus, Synechococcus*) and viruses (Marie et al., 1999).

A 0.45 µm polyethersulfone filter (Supor©) was used to filter samples for Dissolved Organic Matter (DOM) on-line. Within 24 h of collection, all samples were acidified with ultrapure hydrochloric acid (HCl, Merck, 0.1 percent, final pH 2.3) and immediately frozen at -20 °C. The filters were than analyzed at LEMAR laboratory (Brest, France) with size-exclusion chromatography (Huber et al., 2011). DOM includes dissolved oxygen, biopolymers, humic substances and low molecular weight acids and neutrals. DOM data is only available at the fixed observation stations along the transect (S1 to S12 on Fig. 1). An optical package (Eco FLBBCD (fChl, bbp, fC- DOM, and C-Rover); Eco 3X1M sensor) was mounted on the CTD-rosette device to capture optical data along with discrete biogeochemical and diversity measurements (Phytofloat protocole, performed at IMEV laboratory). These measurements were accompanied by discrete sampling (3 depths) of seawater from the Niskin bottles for POC, flow cytometry and polarized microscopy. Pigment concentrations in the SSW from CTD samples were measured using High-Performance Liquid Chromatography (HPLC). Samples of 2.7 L were filtered within 2 h of sampling through 25 mm glass fiber filters (GF/F; Whatman™; 0.7 µm) and filters transferred to cryovials, flash-frozen in liquid nitrogen and stored at -80°C. Filter samples were then processed by the SAPIGH analytical platform at the Institut de la Mer de Villefranche (IMEV, France). For the analytical details on the HPLC analysis please refer to Ras et al., (2008). Diazotroph abundances were also measured from the underway system (Benavides et al., 2021) and CTD casts (Bonnet et al., 2023). Diazotroph abundances were estimated using quantitative PCR (qPCR) targeting the *nifH* gene, which encodes a subunit of the nitrogenase enzyme. Discrete seawater samples (~2 L) were collected either using an automated filtration system (Benavides et al., 2021) or by a peristaltic pump onto 0.2 µm Supor (Cole Parmer, Vernon Hills, IL) filters, frozen in liquid

https://doi.org/10.5194/egusphere-2025-3580
Preprint. Discussion started: 8 August 2025

nitrogen, and stored at -80°C until processed. The DNA extraction was conducted using the method published in Moisander at al. (2008). The abundance of diazotrophs was determined using TaqMan qPCR assays and previously published primer-probe sets for *Trichodesmium,* UCYN-A1, UCYN-B and UCYN-C targeting the *nifH* gene (Church et al., 2005; Thompson et al., 2024).

2.3 Sea spray aerosol characterization

Nascent SSA generated from the underway seawater was also directed to on-line instrumentation for its microphysical and chemical characterization. After passing through a drier, the generated SSA size distribution was analyzed using a Differential Mobility Particle Spectrometer (DMPS) over the particle diameter size range 10-500 nm and using an optical particle spectrometer (OPC) type WELAS over the particle size range 0,5-10 µm, using the same setup as Sellegri et al. (2005).

2.4 INP analysis

INP samples were taken both in the SSA and in the SSW. SSA was sampled for INP analysis using a 4-stage cascade impactor (DEKATI PM10 Impactor) and quartz filters placed on impactor stages, with a time resolution of about 24 hours, due to the scarcity of SSA INPs that was observed in other campaigns using the same setup (e.g. Trueblood et al., 2021). Quartz filters were heated at 800°C for 1 hour under controlled air conditions prior to sampling. Blank samples were taken weekly using the same procedure. INPs were sampled from the UWAY at 4.5 m depth and stored in Falcon tubes. Both filter and SSW samples were immediately stored at -20 °C after sampling.

INP analysis was performed after the campaign on land. INPs were analyzed in both SSA and SSW in the immersion freezing mode using the LED-Based Ice Nucleation Detection Apparatus (LINDA, Stopelli et al., 2014). The operating principle of LINDA is largely described in Stopelli et al., (2014). Briefly, the analysis consists on gradually freezing liquid samples distributed in 52 Eppendorf tubes disposed on a plate placed in a cooling bath (JULABO FP40 thermostat). The temperature is measured using four Pt_{1000} sensors in each corner of the plate, with a precision of 0.1 °C. The tube array was monitored by an USB CMOS Monochrome Camera from 0 °C to -20 °C. Freezing events are detected by a sudden decrease in the transmission of light from a LED array placed below the tubes. INP concentrations as a function of temperature were calculated using the Vali (1971) formula.

For aerosol samples, filter punches (4.3 cm^2 and 4.9 cm^2 respectively for sub- and supermicron samples) were washed in 25 mL of 0.9% NaCl solution for 20 minutes while being agitated. Half of the Eppendorf© tubes (26 tubes) of those samples were filled using the resulting solution. The remaining solution was then heated for 30 minutes at 100 °C in boiling water, before being used to fill the remaining 26 tubes. This heat treatment allows for an estimation of the lowest contribution from biological INPs issued from the comparison of unheated and heated samples (Christner et al., 2008a; Wilson et al., 2015; O'Sullivan et

https://doi.org/10.5194/egusphere-2025-3580
Preprint. Discussion started: 8 August 2025

al., 2018). This procedure is shown in Figure S2. Half of the Eppendorf© tubes were then filled with the untreated sample. The seawater samples were then subjected to the same heat treatment as the filter samples, and the second half of the Eppendorf© tubes was filled using the heated samples (Fig. 2). In order to reach INP concentrations above the limit of detection (LOD), the Eppendorf tubes were filled with 200 µL for seawater samples, and 400 µL for extracted filter samples. For comparison to literature, INP concentrations in SSA were normalized either by the total aerosol surface (surface site density n_S or INP.m^{-2}) of the sea spray generated.

Blank filters were analyzed using the same procedure in order to estimate background errors. On average, blank samples started freezing at around -10 °C, and were below the filter samples until about -18 °C, therefore determining the lower temperature that can be reached with our sampling/analytical procedure. Heated blank samples showed increased IN activity at all temperatures compared to unheated blanks, which hints that the heat treatment results in some contaminated samples. Significant impact of the heating procedure on analysis is seen for temperatures <-17 °C. Sample concentrations were corrected from the average blank value when they were above two standard deviations of the blank samples. Values of the samples that were below this threshold were considered lower than the LOD. The data from seawater samples was shifted by 2 °C to take into account the effect of salinity on the freezing temperature (Doherty et al., 1974). Contrary to filter samples, the seawater samples were not corrected for background, as using a laboratory made solution would induce further errors and hypothesis.

3 Results and discussion

3.1 Biogeochemical properties of the surface seawater

The sampled waters are divided into three zones: the Melanesian waters (MEL), the Lau Basin waters (LAU), and the West Pacific gyre (WGY) waters. The differences in each zone for the available biogeochemical variables measured in the surface seawater are illustrated in Figure 3.

https://doi.org/10.5194/egusphere-2025-3580
Preprint. Discussion started: 8 August 2025

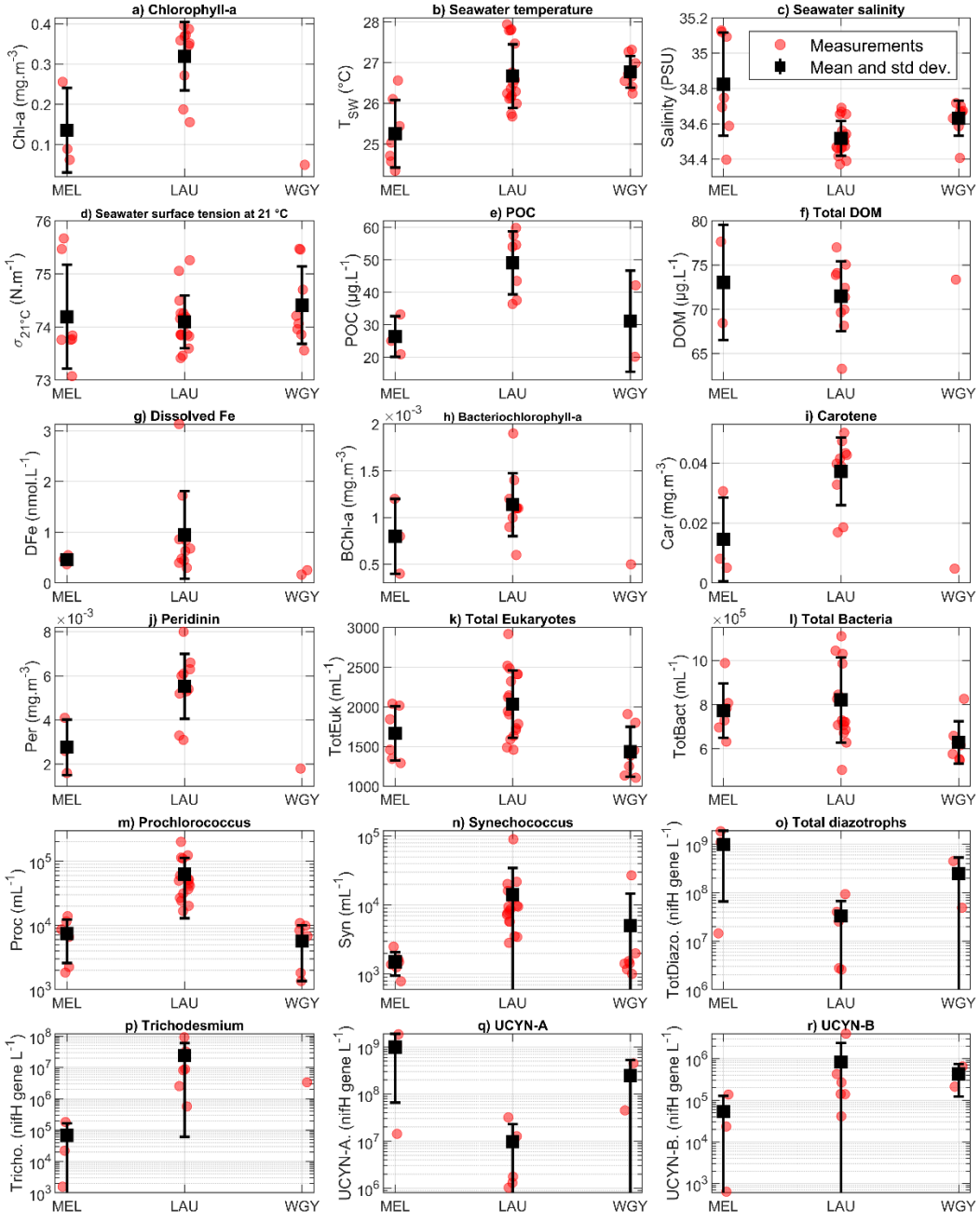

Figure 2 – Summary of surface seawater parameters, separated by type of water (MEL, LAU and WGY) : a) Surface chlorophyll-a (mg.m^{-3}), b) Seawater temperature (°C), c) seawater salinity (PSU), d) seawater surface tension at 21°C (N.m^{-1}), e) particulate organic carbon (µg.L^{-1}), f) dissolved organic matter (µg.L^{-1}), g) dissolved iron (nmol.L^{-1}), h) bacteriochlorophyll-a (mg.m^{-3}), i) carotene (mg.m^{-3}), j) peridinin (mg.m^{-3}), k) total eukaryotes abundance (#.mL^{-1}), l) total bacteria abundance (#.mL^{-1}), m) *Prochlorococcus* abundance (#.mL^{-1}), n) *Synechococcus* abundance (#.mL^{-1}), o) Total diazotrophs abundance (nifH gene.L^{-1}), p) *Trichodesmium* abundance (nifH gene.L^{-1}), q) UCYN-A abundance (nifH gene.L^{-1}), r) UCYN-B abundance (nifH gene.L^{-1}). Standard deviation bars extending below the graph go to zero.

https://doi.org/10.5194/egusphere-2025-3580
Preprint. Discussion started: 8 August 2025

Surface chlorophyll-a concentrations were 3 to 6 times higher in the LAU than in the MEL or WGY zones, with mean values of respectively 0.32±0.085 mg.m^{-3}, 0.136±0.105 mg.m^{-3} and 0.050 mg.m^{-3}, highlighting the increase in biological biomass in the hydrothermally-influenced waters (Fig. 2a). It should be noted that only one measurement is available in the WGY. The seawater temperature (Fig. 2b) was higher in the WGY waters and during the second passing of the LAU, due to the seasonal temperature increase over the cruise period. Salinity and surface tension (Fig. 2c and 2d) were generally lower in the LAU (34.52±0.10 PSU and 74.09±0.50 N.m^{-1}) than in the MEL (34.82±0.29 PSU and 74.19±0.98 N.m^{-1}) and WGY (34.63±0.10 PSU and 74.4±0.73 N.m^{-1}).

Planktonic microorganisms were consistently more abundant in the LAU surface waters compared to those of MEL and WGY. In particular, *Prochlorococcus, Synechococcus* and *Trichodesmium* (Fig. 2n-p) were more than an order of magnitude more abundant in the LAU region than in the two oligotrophic ones. Bacterial abundances exhibited a similar trend but with a lower magnitude (Fig. 2m), with values respectively of 8.21±1.93×10^5 mL^{-1}, 7.73±1.23×10^5 mL^{-1} and 6.29±0.96×10^5 mL^{-1} in the LAU, MEL and WGY. The abundance of eukaryotes (Fig. 2l) almost doubled in the LAU waters compared to the MEL and WGY waters. In contrast to *Trichodesmium*, when summing all diazotrophs together, they were generally more abundant in the MEL (9.9±9.3×10^8 nifHgene.L^{-1}) and WGY (2.5±2.8×10^8 nifHgene.L^{-1}) and less abundant in the LAU (0.3±0.3×10^8 nifHgene.L^{-1}), with differences among groups: UCYN-B and *Trichodesmium* (Fig. 2q, r) where more abundant in LAU waters, while UCYN-A (Fig. 2q) were more abundant in MEL and WGY waters. One caveat is that there are only 2 sampling points in both the MEL and the WGY, which means that interpretations should be made with caution.

POC concentrations (Fig. e) were on average 343.4 ± 9.7 µg.L^{-1} in the LAU waters, with values 4 to 5 higher than in the MEL and WGY waters. Mean DOM concentrations remained constant between regions (Fig. 2f), with values of 71.9 ± 4.0 µg.L^{-1} . Similarly to Chl-a, the other pigments depicted in Fig. 2 (Carotenes, Peridinin, Bacteriochlorophyll-*a* – Fig.2h,i,j) exhibited concentrations 2 to 3 times higher in the LAU than in the MEL and WGY waters.

Overall, most biogeochemical markers exhibited the highest values in the LAU waters, confirming that the LAU waters were mesotrophic waters, rich in biological activity and dissolved iron. The MEL were oligotrophic waters, and WGY were ultra-oligotrophic waters. In the following sections, we explore how INP concentrations vary across the three zones, and the potential relationships between INP and biogeochemical parameters.

https://doi.org/10.5194/egusphere-2025-3580
Preprint. Discussion started: 8 August 2025

3.2 Ice nucleating properties of the surface seawater

3.2.1 General features

The cumulative INP concentrations total and heat stable INP_{SW} measured during the campaign are reported in Fig.3. On average, 10 % of the samples were frozen at −13.0 ± 1.9 °C, 50% of the samples were frozen at −15.5 ± 0.9 °C, and 90% of the samples were frozen at −17.0 ± 1.2 °C. In the following sections, the INP data will be split in three different categories : the total INP data from unheated samples (INP_{tot}), the INP data from heated samples (Heat Stable INPs, or INP_{HS}) and the heat labile INP (INP_{HL}) which is the difference between total and heat stable INPs, and represents proteinaceous INPs (Pummer et al., 2015).

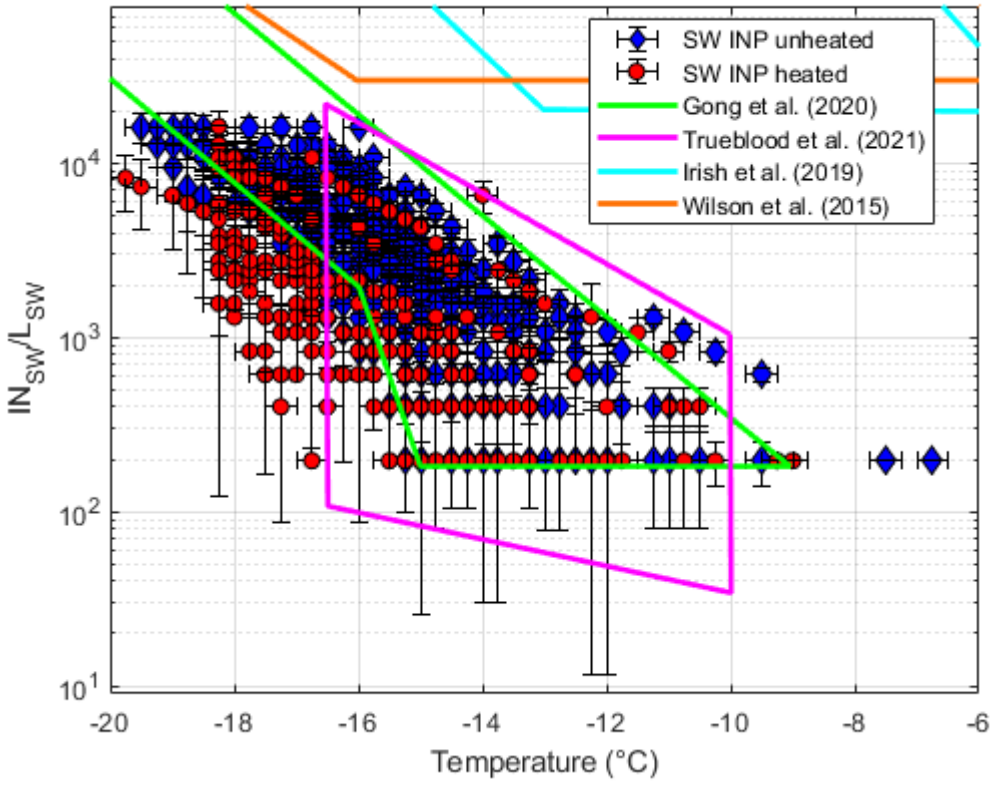

Figure 3 – Cumulative INP concentrations in the SSW as a function of temperature for INP_{tot} and INP_{HS} in comparison to ranges of INP concentrations measured in the SSW in the literature. Data from previous studies includes Gong et al., (2020) at Cabo Verde; Trueblood et al., (2021) in the Mediterranean Sea; Irish et al., (2019b) in the Canadian Arctic and Wilson et al., (2015) in the Arctic, Pacific and Atlantic. Error bars correspond to 3 standard deviations of replicates.

https://doi.org/10.5194/egusphere-2025-3580
Preprint. Discussion started: 8 August 2025

Average total seawater INP concentrations were 490±540 INP.L_{SW}^{-1} , 2000±1500 INP.L_{SW}^{-1} and 7200±4900 INP/L_{SW}^{-1} for INP_{tot} at -13 °C, -15 °C and -17 °C respectively. Similar seawater INP concentrations have been observed in other studies performed in oligotrophic waters (Gong et al., 2020; Trueblood et al., 2021) and of several orders of magnitude lower concentrations than in richer Northern hemisphere seawaters (Irish et al. 2019; Wilson et al. 2015) (see reference lines in Fig. 3). Similarly to other studies in marine environments (eg. Wilson et al., 2015; Irish et al., 2017; McCluskey et al., 2018a), heating the samples results in a clear decrease in INP concentrations. At any given temperature, the fraction of heat-labile INP concentrations represents 63% to 100% (average: 81 ± 11%) of the total INP concentrations. The highest fractions of HL INPs are at temperatures warmer than -14 °C, whereas the lowest fractions are at temperatures between -14 °C and -18 °C. This hints at the presence of a large fraction of heat labile proteinaceous material of biological origin INPs, which are known to be active at warmer temperatures than the heat stable material.

INP concentrations along the transect are shown in Figure 4 for three fixed temperatures, at -13 °C, -15 °C and -17 °C, corresponding to the average T_{10}, T_{50} and T_{90} of the samples. At all temperatures, INP concentrations measured in the LAU waters where 2 to 3 times higher than in the MEL and WGY waters. Thus, INP concentrations follow the trend of most biogeochemical parameters in seawater. This is in line with previous marine studies linking increased plankton biomass with increased INP concentrations in the seawater (e.g. Irish et al., 2017; McCluskey et al., 2018b; Wolf et al., 2020a). Additionally, we investigated the influence of the direct proximity of the Panamax and Simone volcanoes (described in Fig. 1), using samples located in their vicinity (corresponding to Stations 5 and 10). We show in Figure B1 that although the Panamax sample exhibits a similar INP concentration than the average of the campaign, the four Simone samples are consistently higher, by a factor of 2 to 6, than the rest of the campaign, including the LAU samples, underlining the likely influence of hydrothermal emissions on INP concentrations in the seawater.

https://doi.org/10.5194/egusphere-2025-3580
Preprint. Discussion started: 8 August 2025

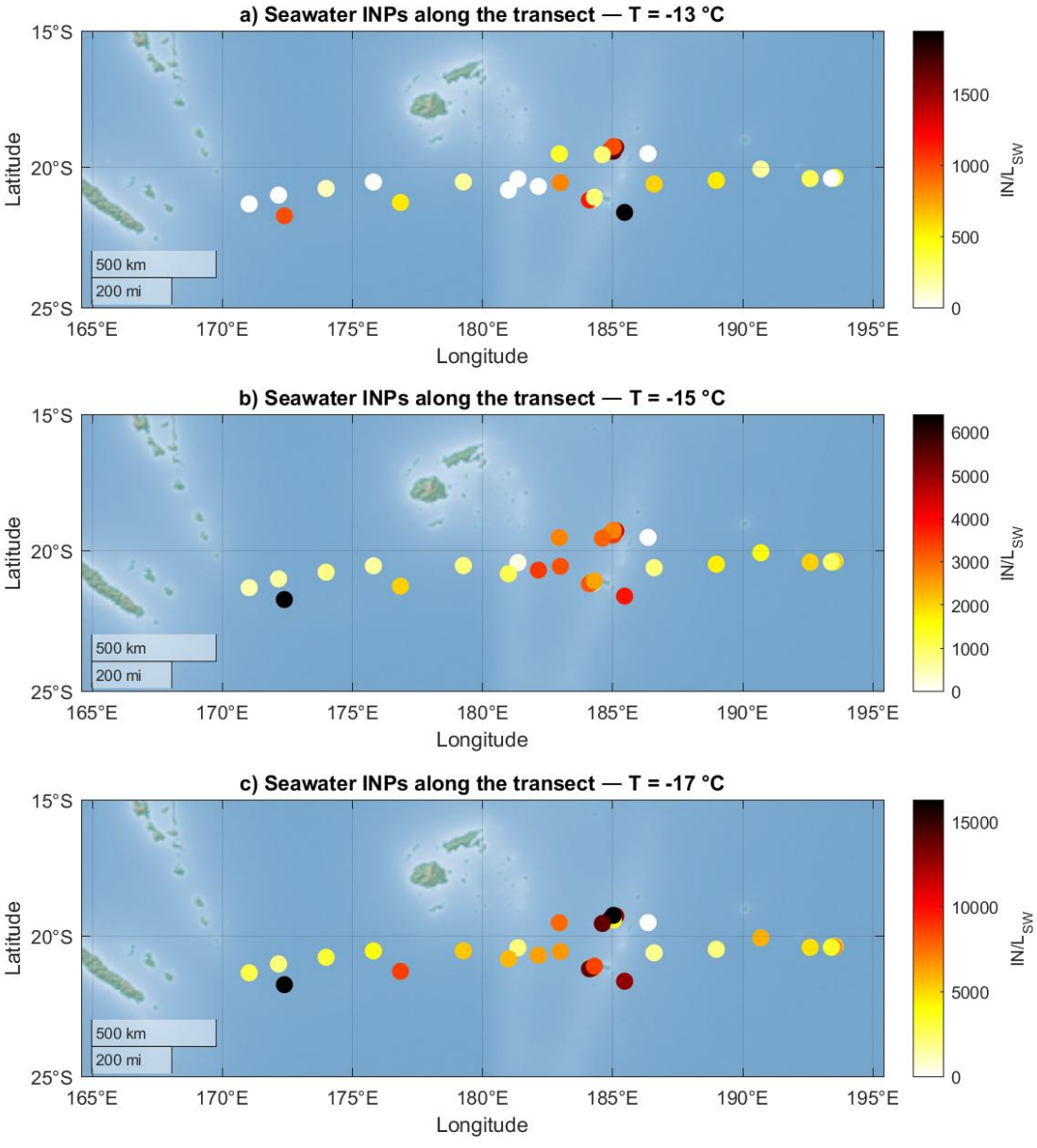

260

Figure 4 – SSW INPs concentrations along the transect, at a) -13 °C, b) -15 °C and c) -17 °C. Colored points represent daily INP concentrations. Map data provided by Esri©.

https://doi.org/10.5194/egusphere-2025-3580
Preprint. Discussion started: 8 August 2025

To further explore the differences between each zone, we show in Figure 6 the seawater INP concentrations in MEL, LAU and WGY at the three temperatures previously defined, for total, heat stable (HS) and heat-labile (HL) INPs. All INP fractions (total, HS and HL) exhibited higher values in the LAU than in the MEL or WGY, indicating an increased contribution of both HL and HS INPS in the LAU zone. However, the difference between LAU and MEL or LAU and WGY is more apparent for heat stable INPs then for heat labile INPs, with an average increase in INP concentrations at all temperatures of 2800±1000 $INP.L_{SW}^{-1}$ for heat stable INPs and 1900±300 $INP.L_{SW}^{-1}$ for heat labile INPs. This was unexpected given the increased biomass measured in the LAU, yet this difference could be explained by an increase in dissolved organic material emitted and produced by the microorganisms stimulated by the hydrothermal activity. This is supported by the fact that heat stable organic matter has been identified as an important contributor to marine INPs activity (e.g. Vergara-Temprado et al., 2017; McCluskey et al., 2018a; McCluskey et al., 2018c; Hill et al., 2023). This hypothesis will be investigated further in the following sections.

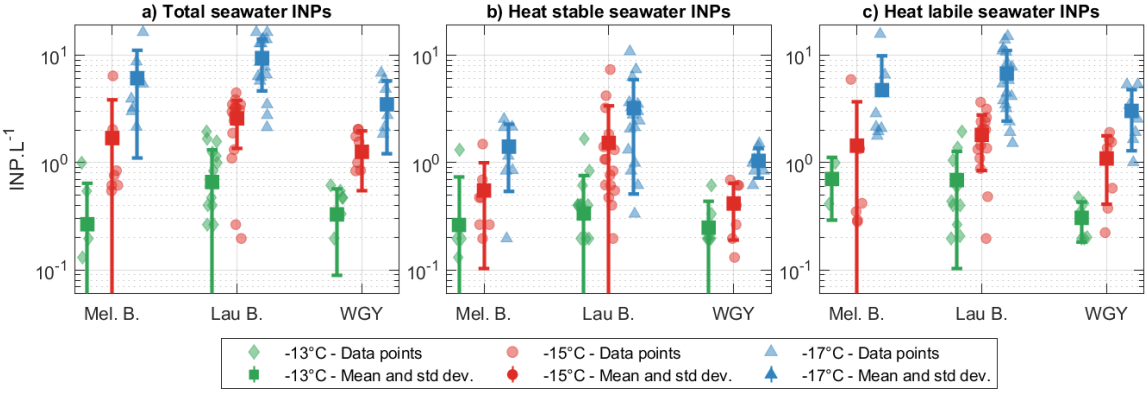

Figure 5 – Swarm plots of seawater INP concentrations in the three identified ocean zones (MEL, LAU and WGY) at −13 °C, −15 °C, and −17 °C : a) total seawater INPs, b) heat stable seawater INPs, c) heat labile seawater INPs. Standard deviation bars extending below the graph go to zero.

3.2.2 Relationships to the seawater biogeochemical properties

A statistical analysis (Peasons's test) was performed on the INP data set over the whole campaign at three different temperatures (-13°C, -15°C ,-17°C), in order to look into the relationships between INP concentrations and the seawater parameters identified in Figure 2. It was not possible to perform this analysis within each ocean zone due to the reduced number of data points. Note that relationships to the surface seawater biogeochemistry were not frequently found for INP concentrations at the warmest temperature (-13°C) compared to relationships at the colder temperatures (-15°C and -17°C), likely a result of low and variable INP concentrations at -13°C.

https://doi.org/10.5194/egusphere-2025-3580
Preprint. Discussion started: 8 August 2025

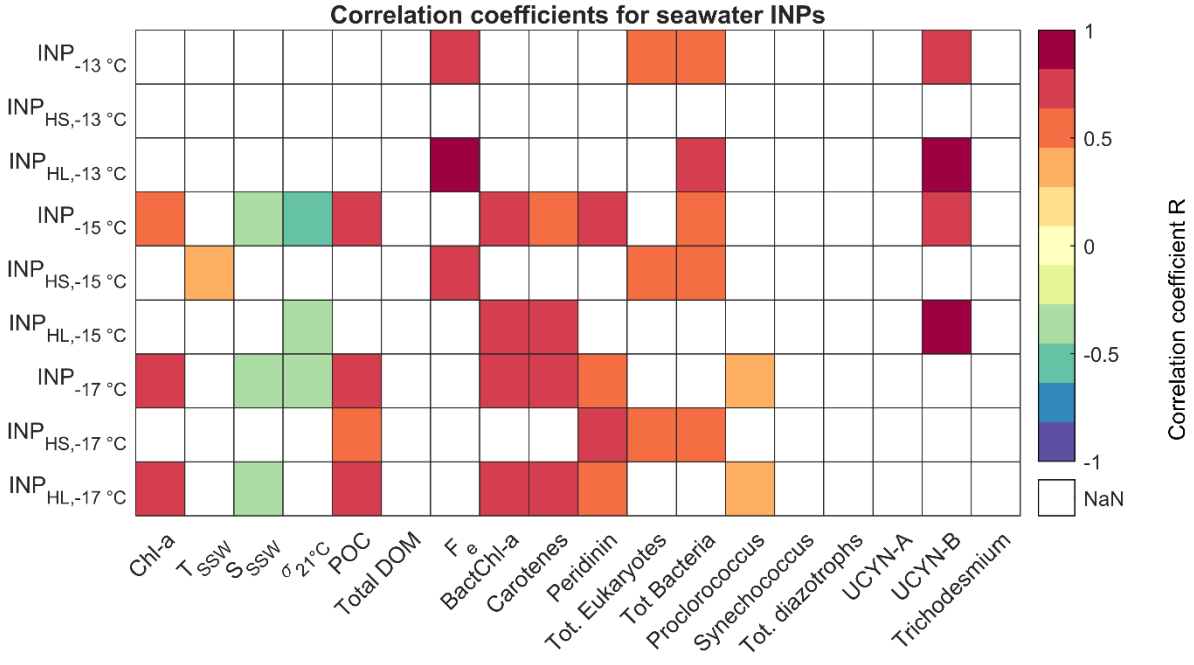

Figure 6 – Linear correlation coefficient R between SSW INP concentrations (total INPs, heat stable INPs and heat labile INPs) at -13 °C, -15 °C and -17 °C and SSW ocean parameters presented in Figure 2. R values are represented as colored cells with values between -1 and +1. White cells represent either empty data points or an insignificant correlation. Significance was determined by Pearson's test, where R associated with p values below 0.05 were noted as significant. The lowest number of points was N = 6, and all R values were computed over 10 to 30 points.

Total INP concentrations at -13°C and -15°C were positively correlated with several biological parameters, such as bacteria (Tot Bact., R≈0.6), pigments (chlorophyll-*a*, Bacteriocholorophyll-*a*, carotenes, peridinin), POC and UCYN-B concentrations. The best correlations were observed with Bacteriocholorophyll-*a* at all temperatures (R>0.7) and carotene at the coldest temperatures (R>0.6), and with UCYN-B (R>0.8) at the warmer temperatures. Bacteriocholorophyll-*a* is a photosynthetic pigment that is linked to light harvesting activity from various phototrophic bacteria (Senge and Smith, 2004; Bryant and Frigaard, 2006). At the coldest temperature (-17°C), total INP vary similarly to *Prochloroccocus* (R≈0.4). This is consistent with the correlation between INP concentrations and carotenes, as *Prochlorococcus* is a prokaryote with α-carotenes (Ralf and Repeta, 1992). Previous studies (eg. Wolf et al., 2019; Hill et al., 2023) have also shown that *Prochlorococcus* could be an effective INP. Similar relationships to Chl-*a* were observed in a mesocosm study on INPs in the SSA, (McCluskey et al., 2018b), where INPs were generally heat-stable and comprised of organic material. Chlorophyll-a is the tracer for the whole phytoplanktonic biomass, (Bryant and Frigaard, 2006; Sinha and Häder, 2008; Foster and Zehr, 2019). Carotenes, and peridinin in particular, are also pigments associated with Chl-*a* as proteins used by dinoflagellates to harvest light (Schulte et al., 2010).

https://doi.org/10.5194/egusphere-2025-3580
Preprint. Discussion started: 8 August 2025

Overall, heat labile INPs had a similar relationship than total INPs with seawater parameters, which is not surprising given the previous observations that they drive the INP population. This suggests that a large part of the INP activity at the warmer temperatures can be explained by the concentration of heat sensitive microorganisms, such as *Prochlorococcus* or UCYN-B, or to products issued from bacterial degradation. Previous studies investigating the link between marine INP concentrations and bacterial abundances have yielded mixed results. Irish et al. (2017) do not report any significant relationship between INPs and bacteria in the Arctic Ocean, but McCluskey et al. (2017) observed that aerosol INPs were positively correlated with aerosolized bacteria.

We also found relationships between heat stable INP and some biological variables. For example, at -15 and -17 °C, heat stable INPs were correlated to total bacteria and total eukaryotes (R≈0.6). Additionally at -15°C, heat stable INPs were correlated with the seawater temperature (R≈0.4) and strongly correlated with dissolved iron (R≈0.8). At -17 °C, they were correlated with POC (R≈0.5) and peridinin (R≈0.7), similarly to total INPs at -17°C.

We observed negative correlations between INPs at -15 °C and -17 °C and salinity, with $R \approx -0.4$ and $p \approx 0.04$, similar to Irish et al. (2017), who observed anticorrelations with $R = -0.7$. Irish et al. (2017) associated this relationship to increased INPs from melting sea ice (associated with lower salinity), which cannot be at the origin of the same relationship observed in the TONGA data set. Furthermore, Irish et al. (2017) reported salinity varying between 28 and 34 PSU, whereas during TONGA, salinity varied from 34 to 35 PSU. Irish et al. (2017) also suggest that a non-colligative effect is not accounted for when correcting for salinity in the seawater samples. However, non-colligative effects have not been previously observed in INP experiments with seawater (Wilson et al., 2015) or sodium chloride solutions (eg. Zobrist et al., 2008; Knopf et al., 2011b). We additionally observed that salinity was negatively correlated with the seawater temperature ($R = -0.75$, $p < 0.005$) and with the total chlorophyll-a concentrations ($R = -0.61$, $p = 0.02$) and carotenes ($R = -0.60$, $p = 0.02$). Hence the anticorrelation between INP and salinity is likely the covariation of biological tracers with seawater salinity.

Organic matter concentration has been linked with INP concentrations in previous studies and has been used in various parameterizations for predicting INP concentrations (e.g. Wilson et al., 2015; Trueblood et al., 2021). Here, we show that both POC and DOC correlate well with INP concentrations at both -15 °C and -17 °C, with $R \approx 0.7$ and p-values below 0.1, but not at -13 °C. Again, this may be due to lower statistics on INP concentrations at this temperature. While POC appear to be better correlated to the total and HL INPs, DOC correlates best with the heat stable fraction of INP, which can be explained by the fact that DOC is often processed by biological and chemical degradation, and is thus a more aged and refractory organic matter than POC. This is in line with the classification proposed by McCluskey et al. (2018b), where DOC- type INPs are more heat stable and POC-type INPs are more heat labile.

In summary, INPs in the seawater during TONGA exhibited significant relationships with biogeochemical properties of seawater. Heat labile INP that represent the majority of the INP population are best correlated to bacteriochlorophyll-a and

https://doi.org/10.5194/egusphere-2025-3580
Preprint. Discussion started: 8 August 2025

bacterial cell abundances, and also to POC. We did not find any significant correlation that could directly link the INP in seawater to volcanic ashes, but INP concentrations were higher in the direct vicinity of underwater volcanoes. This hints that the bacteria themselves or their short-live degradation products are responsible for the ice nucleation activity observed, which is also consistent with POC-type INPs (McCluskey et al., 2018b). This would mean that the impact of hydrothermal activity on INP concentrations is indirect, i.e. related to an increase in dissolved iron that boost phytoplankton abundances, which in turn increases the IN activity of seawater.

3.3 Ice nucleating properties of the nascent sea spray aerosols

INP concentrations in the SSA were measured in two size ranges, submicron (<1 µm, N=13 samples) and supermicron (>1 µm, N=12 samples). For a better comparison to the literature, SSA INP concentrations were normalized to the total surface of SSA aerosols (surface site density n_S, represented in Figure 7), and to the number of SSA aerosols (INP/aer, Figure B2) calculated from the aerosol data presented in Figure A3. Daily SSA concentrations were mostly between 100 and 1500 cm^{-3}, with values above 2000 cm^{-3} reached on the first five days of the campaign. The limit of detection (LOD) was defined as values greater than 2 times the standard deviation of blank concentrations, and values that were below that threshold were set to zero. The n_S values were low and about half of the samples were below the LOD. For the submicron SSA particles ($n_{S,sub}$) 43% of the samples were above the LOD, compared to 50% of the supermicron SSA particles INP ($n_{S,super}$) samples.

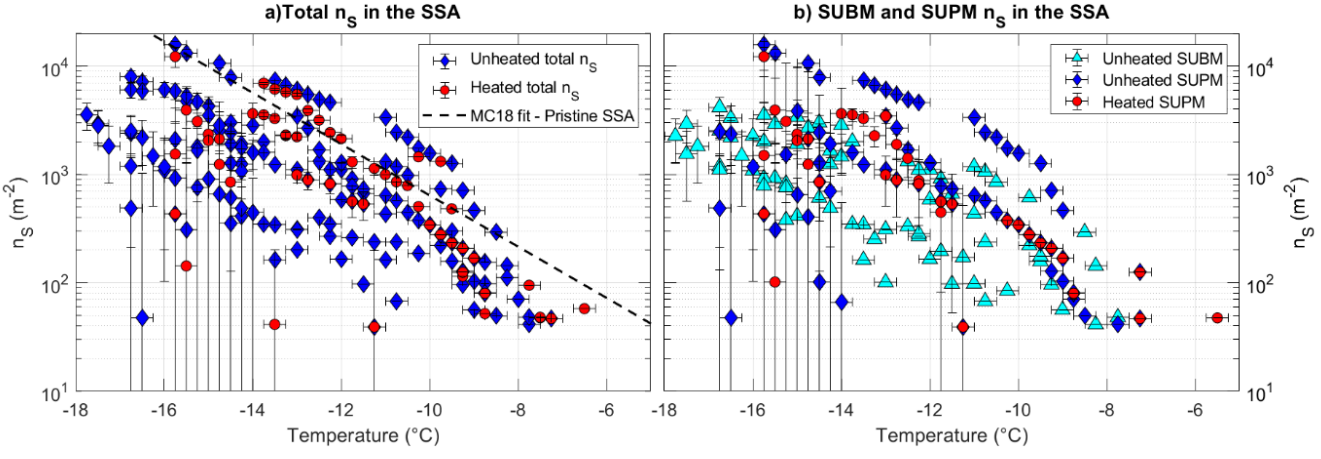

Figure 7 – Nucleation site densities n_S as a function of temperature measured in the SSA. (a) Total unheated and heated n_S and McCluskey et al. (2018c) fit for pristine SSA. Only the samples where both the submicronic and supermicronic n_S are above the LOD are shown. (b) Unheated submicron n_S ($n_{S,sub}$), unheated supermicron n_S ($n_{S,super}$) and heated supermicron n_S. Error bars correspond to three standard deviation of sample blanks. Error bars that go below the plot go to zero, error bars that are not shown are smaller than the markers size.

https://doi.org/10.5194/egusphere-2025-3580
Preprint. Discussion started: 8 August 2025

Total values of n_S were in the range of 10^1–10^2 m^{-2} at -8°C and 10^3–10^{-4} m^{-2} at -17 °C, i.e. 1 to 2 orders of magnitude lower than n_S fitted for ambient marine aerosols sampled in the North Atlantic coastal research station Mace Head by McCluskey et al. (2018c) (MC18, shown in Fig. 7a), and than values measured using artificially generated SSA in the Gulf of Mexico (Córdoba et al., 2025). This is in line with McCluskey et al. (2018a), who concluded that INP concentrations in the southern hemisphere were generally lower than those of the northern hemisphere. INP/aer concentrations measured at -18°C during TONGA are in the range of 10^{-7} to 10^{-8} INP.aer^{-1}, i.e. one to two orders of magnitude higher than INP/aer concentrations reported for SSA generated from oligotrophic waters in the Mediterranean Sea, that were measured in the range of 10^{-9}INP aer^{-1} (Trueblood et al., 2021). An interesting observation is that the INP/aer are similar for both submicron aerosol particles and supermicron aerosols over the studied temperature range showing that the high numbers of submicron particles can compensate for their low surface area in terms of INP activity.

On average across all temperatures, supermicron $n_{S,super}$ represented the minority of total n_S, with a fraction of 41±18%. This is especially the case at the warmer temperatures, where this fraction reaches 16±21% at -13°C (Fig. 8a). The fraction of supermicron n_S was highest at -15 °C, with a value of 68±33%. Fractions of heat labile INPs were also very different between the submicron and supermicron size ranges. In the submicron size range, all of $n_{S,sub}$ are heat labile, suggesting that their INP activity is driven by the smaller heat labile organic material ejected as film drops. It is well know that the submicron marine aerosol population is dominated by organic material (Freney et al., 2020). On the other hand, only 20% of INPs in the supermicron size range are heat labile on average (Figure 7b and 8b), indicating that they could be larger particles whose IN activity is likely a result of dissolved organic carbon mainly composed of processed heat stable carbon. This observation contrasts with that made by McCluskey et al. (2018b), who categorized INP in two classes: INPs smaller than 0.2 µm that were mostly heat stable, and INPs larger than 0.2 µm that were mostly heat labile. However, we chose to separate the INPs at the size cutoff of 1 µm, where a larger difference in aerosol chemical properties is often observed as a result of differences in sea spray production mechanisms (film vs jet drops, De Leeuw et al.; 2011).

https://doi.org/10.5194/egusphere-2025-3580
Preprint. Discussion started: 8 August 2025

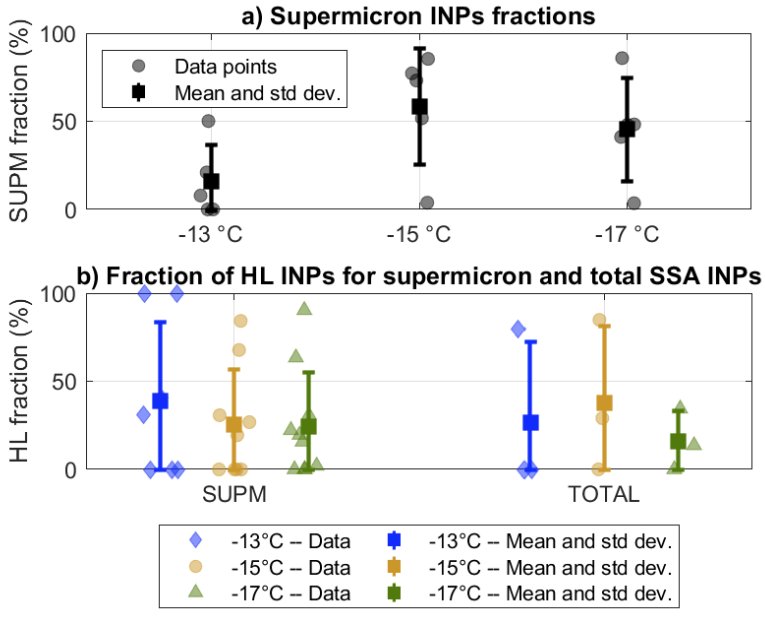

Figure 8 – a) Fraction of supermicron INPs in the SSA at -13 °C, -15 °C and -17 °C, b) Fraction of heat labile INPs for supermicron and total SSA INPs at -13 °C, -15 °C and -17 °C. Points represent data points (each corresponding to one day of sampling) and error bars represent mean and standard deviations of the data points.

Surface site density n_s were averaged for each geographical zone (LAU, MEL and WGY) for comparison (Fig. 9). While average total n_s cannot be distinguished between the LAU region and the two oligotrophic zones, heat stable total n_s (Fig 9b) and submicron n_s (Fig. 9c) were on average higher in the LAU than in the WGY at all temperatures. These observations are in line with those in the SW, as INP_{SW} were enriched in the LAU compared to the MEL and WGY, and predominantly from heat stable INPs at the warmest temperature. This would point to INP_{SW} influenced by hydrothermal sources being preferentially transferred to the sea spray in the form of heat stable supermicron particles in the LAU zone (hence likely via the ejection of jet drops rather than film drops). We also represent in Fig. 10 the n_S spectra of LAU samples and MEL+WGY samples, confirming that n_S in the hydrothermal-influenced area was generally higher than in both oligotrophic zones for the warmest freezing temperatures, although the samples exhibited large variations within a single zone. In particular, supermicron n_s on the 10th Nov 2019 exhibited values significantly (3 standard deviations) higher than the average supermicron concentrations. While this increase was not linked to significant variations in the seawater parameters presented in Fig. 2, it was sampled directly in the vicinity of the Panamax Volcano (Fig. 1). However, this increase is not observed near the Simone Volcano like for INP_{SW}, but this nonetheless suggests that hydrothermal emissions may boost SSA INPs activity, particularly through an increase in larger heat stable INPs.

https://doi.org/10.5194/egusphere-2025-3580
Preprint. Discussion started: 8 August 2025

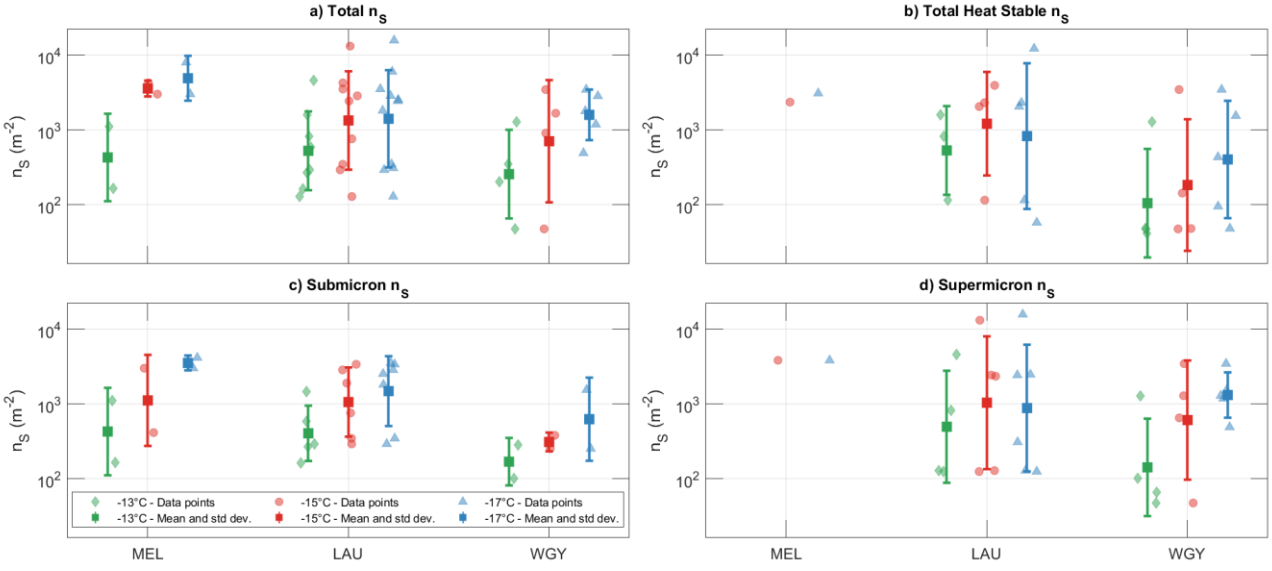

Figure 9. Sea spray aerosols ns in the three identified ocean zones at −12 °C, −15 °C and −17 °C : a) Total SSA INPs, b) Heat Stable SSA INPs, c) Submicron SSA INPs, d) Supermicron SSA INPs.

We investigated correlations between INP concentrations in the SW and n_S in the SSA at each temperature, for each of the three INP_{SSA} datasets (submicron, supermicron, total). Correlations were not significant, presumably because the INP_{SSA} data is too scarce for reliable statistical relationships. In order to predict sea spray ns properties from biologically-driven seawater INP concentrations in atmospheric models, we calculated the transfer function from seawater INP to SSA INP. The transfer function of seawater INPs to SSA INPs, defined as the ratio $n_s \,/\, INP_{sw}$ was calculated for total, heat stable and heat labile INPs. On average between -12 and -17 °C, we report median values of 1.72 (interquartile range: [1.15-3.32]) $m^{-2}.L_{SW}$ for total INPs. This value was similar for heat labile INPs (1.70 [0.96-2.42] $m^{-2}.L_{SW}$), but was doubled for heat stable INPs (3.30 [1.37-5.56] $m^{-2}.L_{SW}$). We do not report significant differences between each ocean zones. Thus, we surmise that heat stable INPs, presumed associated to jet drops were more efficiently transported to the SSA than heat labile INPs, presumed associated to film drops.

4. Conclusions

Daily INP concentrations were measured in both surface seawater and in artificially generated SSA from an underway seawater (5 m depth) in the region of the Tonga-Kermadec volcanic arc together with a range of other biogeochemical parameters, providing a unique opportunity to investigate the potential impact of ocean biological properties on the INP variability.

We show that INPs in the bulk surface seawater were generally active at temperatures <-12 °C, indicative of the presence of ice nucleating biological material, which was confirmed by the high fraction of heat labile INP. The INP concentrations in the

https://doi.org/10.5194/egusphere-2025-3580
Preprint. Discussion started: 8 August 2025

surface seawater measured during TONGA were overall lower than reported from biologically richer seawaters (Wilson et al., 2015; Irish et al., 2017), but were comparable to other oligotrophic regions (McCluskey et al., 2018a; Trueblood et al., 2021). Surface seawater INP concentrations were about two-fold higher in the mesotrophic Lau basin compared to the oligotrophic Melanesian Basin waters and the ultra-oligotrophic West Pacific Gyre waters at all freezing temperatures, consistent with higher biological activity, and higher abundances of microorganisms such as *Prochlorococcus*, chlorophyl-a and carotenes, and POC in the Lau basin (e.g. Moutin et al., 2018; Bonnet et al., 2023; Mériguet et al., 2024). Over the whole campaign, medium to strong correlations were found between INP_{SW} concentrations and photosynthetic pigments (notably bacteriochlorophyll-a and carotene), bacterial abundance and POC ($0.6 < R < 0.8$), suggesting that the INP variability, and especially the heat labile fraction, was driven by the POC-type INPs as assumed by McCluskey et al. (2018b). The heat stable fraction of INP_{SW} exhibited correlations with the DOC and were not as variable as the heat labile INP_{SW}. One hypothesis is that the variability of INP is driven by POC, and this variability would add to a constant pool of the DOC type INP always present and more constant.

The nascent SSA generated from these seawaters exhibited generally low n_S values compared to other marine regions, which is consistent with other observations in the Southern Ocean (McCluskey et al., 2018a). In agreement with the INP_{SW}, SSA n_S were mostly heat labile and therefore likely to be of biological/organic origin. Submicron SSA n_S represented on average the majority of SSA INPs, although this was variable depending on the temperature. Submicron n_S were all heat labile while supermicron n_S were mainly heat stable, showing that submicron n_s was likely the result of small heat labile POC via the ejection of film drops, while supermicron n_s were more likely to be caused by heat stable DOC ejected in the form of jet drops. Supermicron INPs were generally more abundant in the nutrient-rich Lau basin, while submicron INPs did not exhibit a significant difference between the oligotrophic waters and the Lau basin. Although no significant correlation was found between SSA n_S and surface seawater INP_{SW} due to too few samples available in the SSA, the general observation of increased concentrations in the Lau basin was coherent with the same trend in the surface seawater. We provide a transfer function linking SW and SSA INPs, evaluated at 1.70 $m^{-2}.L_{SW}$ over the whole transect. This value was however doubled for heat stable INPs, hinting that heat stable INPs were more efficiently transferred from the seawater to the SSA in the form of jet drops.

Our observations suggest that the hydrothermal emissions do not have any direct effect on the composition or properties of the INPs, but rather an indirect effect through the stimulation of biological activity, that, in turn, influences IN properties. This result highlights the importance of studying the marine IN activity along trophic gradients in contrasted waters, especially in regions influenced by hydrothermal activity. Such regions include the Tropical Ocean and the Southern Ocean where measurements are scarce. Combining INP measurements in the seawater and SSA with various biogeochemical measurements allows for a better understanding of the nature of marine INPs, and thus help improve atmospheric models that predict the formation of clouds over pristine marine environments.

https://doi.org/10.5194/egusphere-2025-3580
Preprint. Discussion started: 8 August 2025

Appendix

Appendix A: Methods

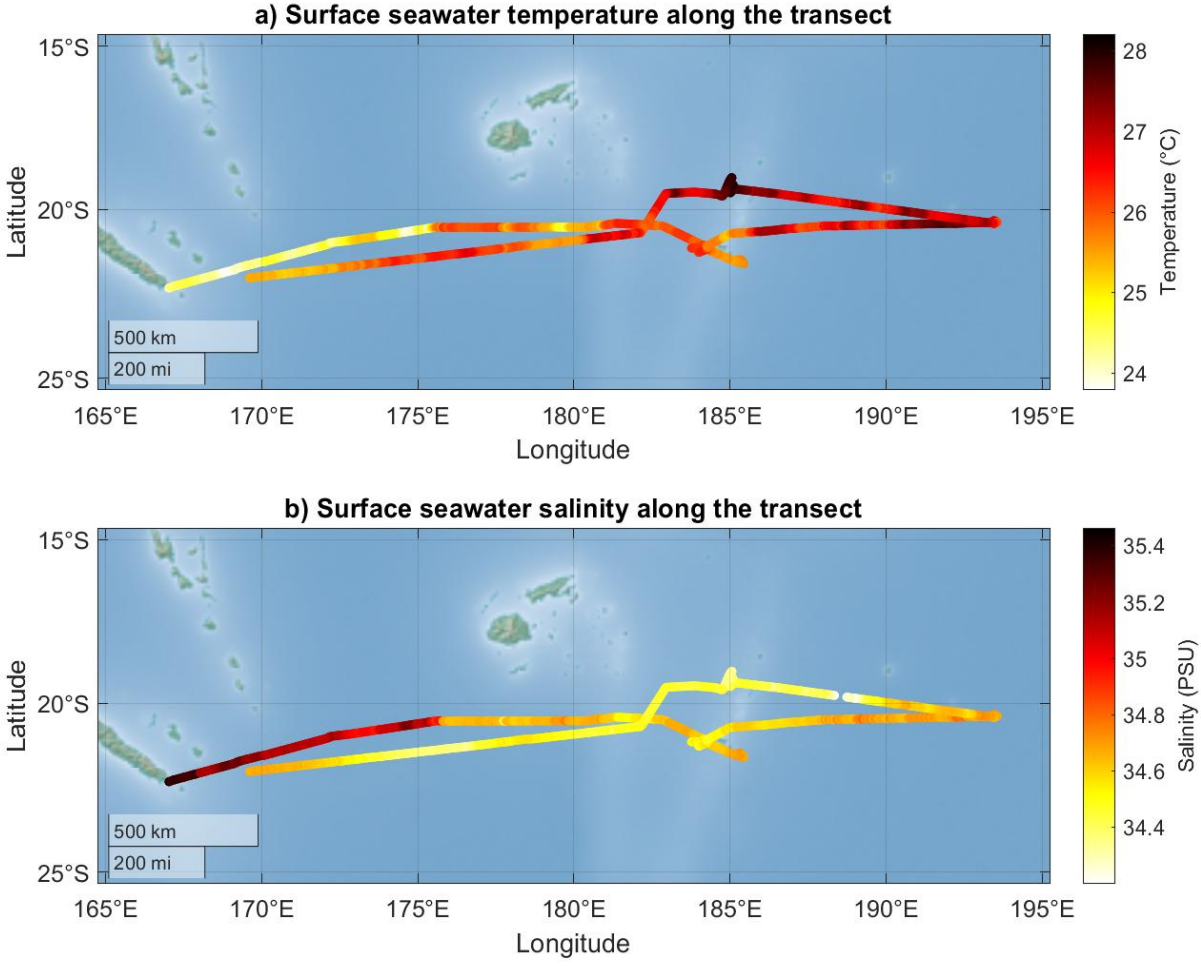

Figure A1 : Surface seawater salinity and temperature along the transect. Map data provided by Esri©.

https://doi.org/10.5194/egusphere-2025-3580
Preprint. Discussion started: 8 August 2025

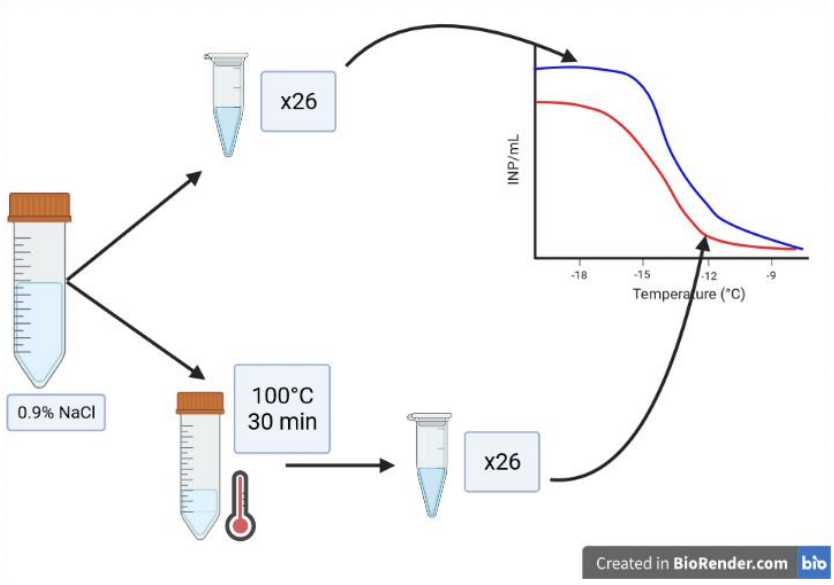

Figure A2 – Schematics of the LINDA analysis of the samples. The blue and red curves on the top right are the cumulative INP concentrations per mL of solution used for analysis, corresponding respectively to the unheated and heated samples. These INP concentrations are calculated using Vali (1971) formula.

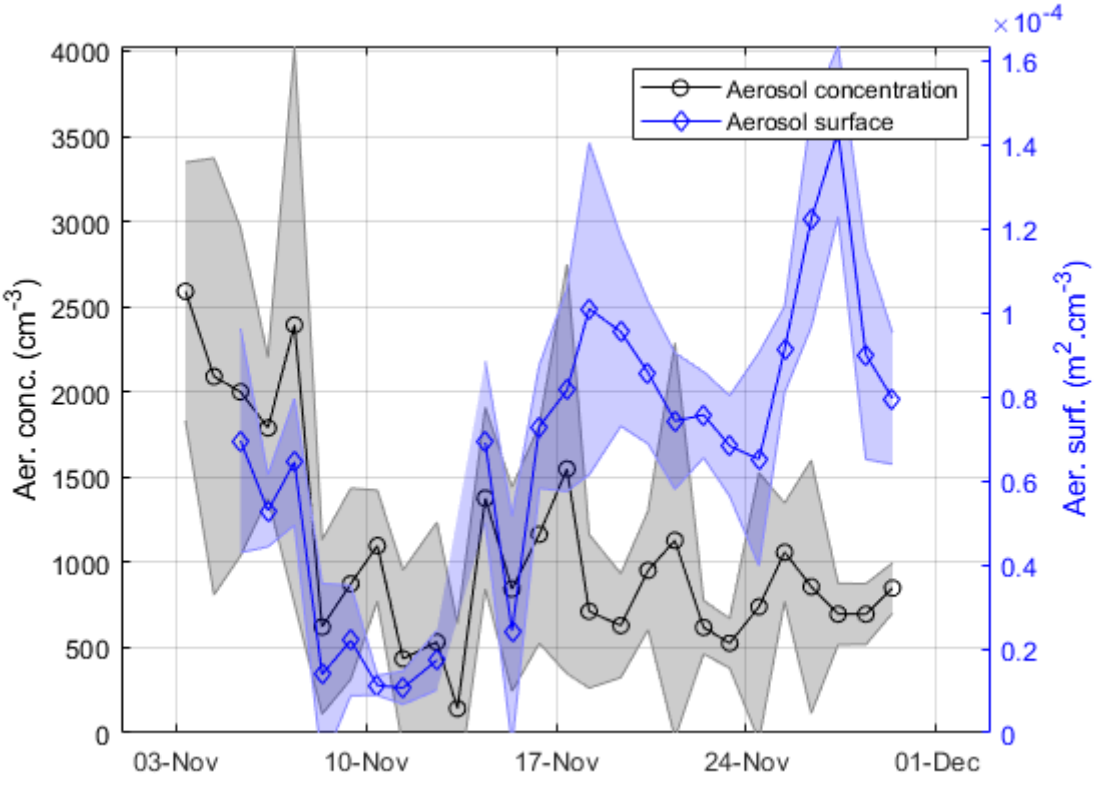

455

https://doi.org/10.5194/egusphere-2025-3580
Preprint. Discussion started: 8 August 2025

Figure A3 – Daily average generated SSA concentration and surface. Shaded area correspond to one standard deviation.

Appendix B: INP measurements

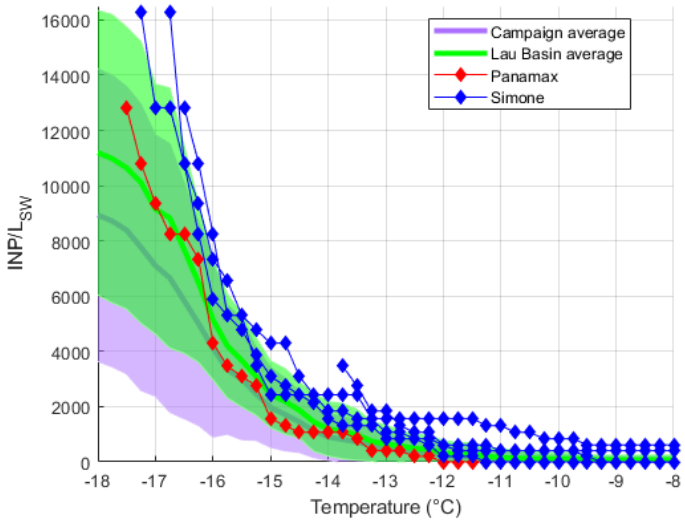

Figure B1 – Comparison of seawater INPs near the Panamax (Station 5) and Simone (Station 10) volcanoes. The campaign and Lau basin averages are represented as purple and green shaded areas (solid line : mean, shaded area : standard deviation of the dataset). Panamax and Simone data are represented as single days INP spectra, corresponding to days where seawater was sampled in the immediate vicinity of the volcano (<20 km distance). This represents one sample for Panamax and four samples for Simone.

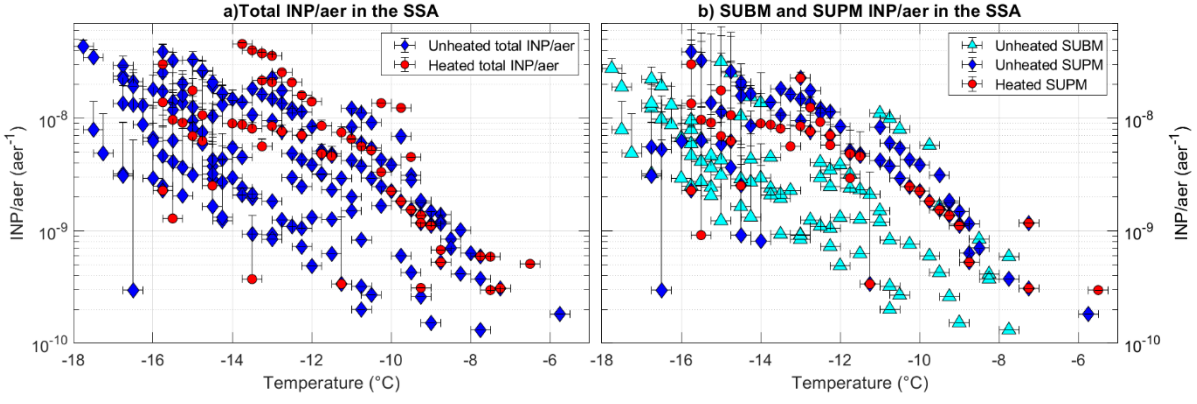

Figure B2 – Cumulative INP/aer concentrations in the SSA for a) Total unheated and heated INP/aer in the SSA; b) Submicronic unheated INP/aer and Supermicronic unheated and heated INP/aer. Error bars are defined by three standard deviation of blank samples.

https://doi.org/10.5194/egusphere-2025-3580
Preprint. Discussion started: 8 August 2025

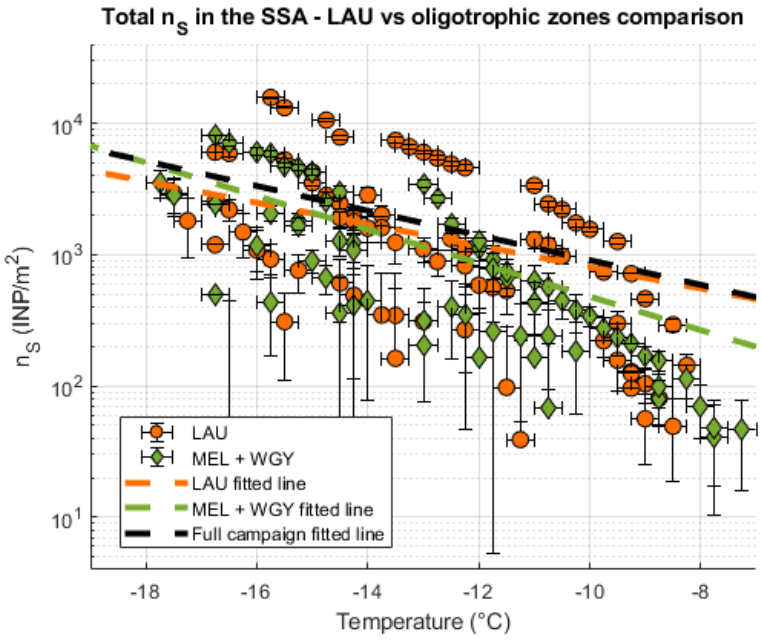

Figure B3 : Comparison of total n_S as a function of temperature in the LAU and MEL+WGY combined, with the associated lines of best fit $n_S(T) = a \cdot exp(bT)$. The Line of best fit for the full campaign is shown as the black dashed line. The fit coefficients are respectively a = 122.8 and b = -0.1879 for LAU, a = 25.38 and b = -0.2938 for MEL+WGY, and a = 104.1 and b = -0.2166 for the full campaign.

Data availability

The data reported in this study are available at https://www.obs-vlfr.fr/proof/php/TONGA/x_datalist_1.php?xxop=tonga&xxcamp=tonga. Ice Nucleating particles data are available at https://doi.org/10.5281/zenodo.16420844.

https://doi.org/10.5194/egusphere-2025-3580
Preprint. Discussion started: 8 August 2025

Author contributions

KS and EF designed the experiments, SB and CG designed and coordinated the TONGA ship campaign. MR and LB prepared the experimental gear. KS performed the sea spray generation experiment and INP sampling, YB analyzed INP concentrations. MB, EB, GD, CD, CG and SB sampled and analyzed seawater biogeochemical parameters. YB prepared the manuscript with contributions from EF, MB, CG, SB and KS.

Competing interest

The authors declare that they have no conflict of interest.

Acknowledgments

This research received funding from the European Research Council (ERC) Sea2Cloud under the Horizon 2020 research and innovation program (Grant agreement number - 771369. Sea2Cloud is endorsed by SOLAS. We thank Véronique Pont (LAERO) for the chemical analysis of the sea spray aerosol. Phytoplankton pigment analyses were performed at the SAPIGH (Service Analytique de Pigments par HPLC) analytical service hosted at the Institut de la Mer de Villefranche (IMEV) and labelled by CNRS INSU. TONGA was funded by Agence Nationale de Recherche grant ANR-18-CE01-0016, A-MIDEX (Excellence Initiative of Aix-Marseille University, a French “Investissements d'Avenir" program). Institut National des Sciences de l’Univers Les Enveloppes Fluides et l’Environnement, TGIR Flotte océanographique française, the Institut de recherche pour le Développement (IRD).

References

Aller, J. Y., Kuznetsova, M. R., Jahns, C. J., & Kemp, P. F. (2005). The sea surface microlayer as a source of viral and bacterial enrichment in marine aerosols. *Journal of Aerosol Science*, *36*(5-6), 801-812. https://doi.org/10.1016/j.jaerosci.2004.10.012

Benavides, M., Conradt, L., Bonnet, S., Berman-Frank, I., Barrillon, S., Petrenko, A., & Doglioli, A. (2021a). Fine-scale sampling unveils diazotroph patchiness in the South Pacific Ocean. *ISME Communications*, *1*(1), 3. https://doi.org/10.1038/s43705-021-00006-2

Benavides, M., Conradt, L., Bonnet, S., Berman-Frank, I., Barrillon, S., Petrenko, A., & Doglioli, A. (2021b). Fine-scale sampling unveils diazotroph patchiness in the South Pacific Ocean. *ISME Communications*, *1*(1), 3. https://doi.org/10.1038/s43705-021-00006-2

https://doi.org/10.5194/egusphere-2025-3580
Preprint. Discussion started: 8 August 2025

Bonnet, S., Benavides, M., Le Moigne, F. A. C., Camps, M., Torremocha, A., Grosso, O., Dimier, C., Spungin, D., Berman-Frank, I., Garczarek, L., & Cornejo-Castillo, F. M. (2023). Diazotrophs are overlooked contributors to carbon and nitrogen export to the deep ocean. *The ISME Journal*, *17*(1), 47-58. https://doi.org/10.1038/s41396-022-01319-3

Bonnet, S., Caffin, M., Berthelot, H., Grosso, O., Benavides, M., Helias-Nunige, S., Guieu, C., Stenegren, M., & Foster, R. A. (2018). In-depth characterization of diazotroph activity across the western tropical South Pacific hotspot of N₂ fixation (OUTPACE cruise). *Biogeosciences*, *15*(13), 4215-4232. https://doi.org/10.5194/bg-15-4215-2018

Bonnet, S., Caffin, M., Berthelot, H., & Moutin, T. (2017). Hot spot of N_2 fixation in the western tropical South Pacific pleads for a spatial decoupling between N_2 fixation and denitrification. *Proceedings of the National Academy of Sciences*, *114*(14). https://doi.org/10.1073/pnas.1619514114

Bonnet, S., Guieu, C., Taillandier, V., Boulart, C., Bouruet-Aubertot, P., Gazeau, F., Scalabrin, C., Bressac, M., Knapp, A. N., Cuypers, Y., González-Santana, D., Forrer, H. J., Grisoni, J.-M., Grosso, O., Habasque, J., Jardin-Camps, M., Leblond, N., Le Moigne, F. A. C., Lebourges-Dhaussy, A., … Tilliette, C. (2023a). Natural iron fertilization by shallow hydrothermal sources fuels diazotroph blooms in the ocean. *Science*, *380*(6647), 812-817. https://doi.org/10.1126/science.abq4654

Bonnet, S., Guieu, C., Taillandier, V., Boulart, C., Bouruet-Aubertot, P., Gazeau, F., Scalabrin, C., Bressac, M., Knapp, A. N., Cuypers, Y., González-Santana, D., Forrer, H. J., Grisoni, J.-M., Grosso, O., Habasque, J., Jardin-Camps, M., Leblond, N., Le Moigne, F. A. C., Lebourges-Dhaussy, A., … Tilliette, C. (2023b). Natural iron fertilization by shallow hydrothermal sources fuels diazotroph blooms in the ocean. *Science*, *380*(6647), 812-817. https://doi.org/10.1126/science.abq4654

Bras, Y., Freney, E., Canzi, A., Amato, P., Bouvier, L., Pichon, J., Picard, D., Minguillón, M. C., Pérez, N., & Sellegri, K. (2024). Seasonal Variations, Origin, and Parameterization of Ice-Nucleating Particles at a Mountain Station in Central France. *Earth and Space Science*, *11*(6), e2022EA002467. https://doi.org/10.1029/2022EA002467

Brooks, S. D., & Thornton, D. C. O. (2018). Marine Aerosols and Clouds. *Annual Review of Marine Science*, *10*(1), 289-313. https://doi.org/10.1146/annurev-marine-121916-063148

Bryant, D. A., & Frigaard, N.-U. (2006). Prokaryotic photosynthesis and phototrophy illuminated. *Trends in Microbiology*, *14*(11), 488-496. https://doi.org/10.1016/j.tim.2006.09.001

Burrows, S. M., Hoose, C., Pöschl, U., & Lawrence, M. G. (2013). Ice nuclei in marine air : Biogenic particles or dust? *Atmospheric Chemistry and Physics*, *13*(1), 245-267. https://doi.org/10.5194/acp-13-245-2013

Christner, B. C., Morris, C. E., Foreman, C. M., Cai, R., & Sands, D. C. (2008). Ubiquity of Biological Ice Nucleators in Snowfall. *Science*, *319*(5867), 1214-1214. https://doi.org/10.1126/science.1149757

Church, M. J., Short, C. M., Jenkins, B. D., Karl, D. M., & Zehr, J. P. (2005). Temporal Patterns of Nitrogenase Gene (*nifH*) Expression in the Oligotrophic North Pacific Ocean. *Applied and Environmental Microbiology*, *71*(9), 5362-5370. https://doi.org/10.1128/AEM.71.9.5362-5370.2005

Cochran, R. E., Laskina, O., Trueblood, J. V., Estillore, A. D., Morris, H. S., Jayarathne, T., Sultana, C. M., Lee, C., Lin, P., Laskin, J., Laskin, A., Dowling, J. A., Qin, Z., Cappa, C. D., Bertram, T. H., Tivanski, A. V., Stone, E. A., Prather, K. A., &

https://doi.org/10.5194/egusphere-2025-3580
Preprint. Discussion started: 8 August 2025

Grassian, V. H. (2017). Molecular Diversity of Sea Spray Aerosol Particles : Impact of Ocean Biology on Particle Composition and Hygroscopicity. *Chem*, *2*(5), 655-667. https://doi.org/10.1016/j.chempr.2017.03.007

Córdoba, F., Ramírez-Romero, C., Cabrera, D., Raga, G. B., Miranda, J., Alvarez-Ospina, H., Rosas, D., Figueroa, B., Kim, J. S., Yakobi-Hancock, J., Amador, T., Gutierrez, W., García, M., Bertram, A. K., Baumgardner, D., & Ladino, L. A. (2021). Measurement report : Ice nucleating abilities of biomass burning, African dust, and sea spray aerosol particles over the Yucatán Peninsula. *Atmospheric Chemistry and Physics*, *21*(6), 4453-4470. https://doi.org/10.5194/acp-21-4453-2021

Cunliffe, M. (s. d.). *Guide to best practices to study the ocean's surface*. 118.

De Leeuw, G., Andreas, E. L., Anguelova, M. D., Fairall, C. W., Lewis, E. R., O'Dowd, C., ... & Schwartz, S. E. (2011). Production flux of sea spray aerosol. *Reviews of Geophysics*, *49*(2).

DeMott, P. J., Hill, T. C. J., McCluskey, C. S., Prather, K. A., Collins, D. B., Sullivan, R. C., Ruppel, M. J., Mason, R. H., Irish, V. E., Lee, T., Hwang, C. Y., Rhee, T. S., Snider, J. R., McMeeking, G. R., Dhaniyala, S., Lewis, E. R., Wentzell, J. J. B., Abbatt, J., Lee, C., … Franc, G. D. (2016). Sea spray aerosol as a unique source of ice nucleating particles. *Proceedings of the National Academy of Sciences*, *113*(21), 5797-5803. https://doi.org/10.1073/pnas.1514034112

Doherty', B. T., & Kester, D. R. (s. d.). Freezing Point ofSeawater'. *Journal of Marine Research*, 17.

Durant, A. J., Shaw, R. A., Rose, W. I., Mi, Y., & Ernst, G. G. J. (2008). Ice nucleation and overseeding of ice in volcanic clouds. *Journal of Geophysical Research*, *113*(D9), D09206. https://doi.org/10.1029/2007JD009064

Fornea, A. P., Brooks, S. D., Dooley, J. B., & Saha, A. (2009). Heterogeneous freezing of ice on atmospheric aerosols containing ash, soot, and soil. *Journal of Geophysical Research*, *114*(D13), D13201. https://doi.org/10.1029/2009JD011958

Foster, R. A., & Zehr, J. P. (2019). Diversity, Genomics, and Distribution of Phytoplankton-Cyanobacterium Single-Cell Symbiotic Associations. *Annual Review of Microbiology*, *73*(1), 435-456. https://doi.org/10.1146/annurev-micro-090817-062650

Freney, E., Sellegri, K., Nicosia, A., Trueblood, J. T., Rinaldi, M., Williams, L. R., ... & Guieu, C. (2020). Mediterranean nascent sea spray organic aerosol and relationships with seawater biogeochemistry. *Atmospheric Chemistry and Physics Discussions*, *2020*, 1-23.

Genareau, K., Cloer, S., Primm, K., Tolbert, M., & Woods, T. (2018). Compositional and Mineralogical Effects on Ice Nucleation Activity of Volcanic Ash. *Atmosphere*, *9*(7), 238. https://doi.org/10.3390/atmos9070238

Gong, X., Wex, H., van Pinxteren, M., Triesch, N., Fomba, K. W., Lubitz, J., Stolle, C., Robinson, T.-B., Müller, T., Herrmann, H., & Stratmann, F. (2020). Characterization of aerosol particles at Cabo Verde close to sea level and at the cloud level – Part 2 : Ice-nucleating particles in air, cloud and seawater. *Atmospheric Chemistry and Physics*, *20*(3), 1451-1468. https://doi.org/10.5194/acp-20-1451-2020

Guieu, C., Bonnet, S., Abadou, F., Alliouane, S., Arnaud-Haond, S., Arnone, V., Baudoux, A.-C., Baumas, C., Beillard, L., Benavides, M., Berman-Frank, I., Bhairy, N., Bigeard, E., Boulart, C., Bouruet-Aubertot, P., Boyd, P., Bressac, M., Camps, M., Chaffron, S., … Whitby, H. (2022). *BIOGEOCHEMICAL dataset collected during the TONGA cruise* [Jeu de données]. SEANOE. https://doi.org/10.17882/88169

https://doi.org/10.5194/egusphere-2025-3580
Preprint. Discussion started: 8 August 2025

GUIEU Cécile & BONNET Sophie. (2019). *TONGA 2019 cruise,L'Atalante R/V*. Sismer. https://doi.org/10.17600/18000884

Hill, T. C. J., Malfatti, F., McCluskey, C. S., Schill, G. P., Santander, M. V., Moore, K. A., Rauker, A. M., Perkins, R. J., Celussi, M., Levin, E. J. T., Suski, K. J., Cornwell, G. C., Lee, C., Del Negro, P., Kreidenweis, S. M., Prather, K. A., & DeMott, P. J. (2023). Resolving the controls over the production and emission of ice-nucleating particles in sea spray. *Environmental Science: Atmospheres*, *3*(6), 970-990. https://doi.org/10.1039/D2EA00154C

Hobbs, P. V., Bluhm, G. C., & Ohtake, T. (1971). Transport of ice nuclei over the north pacific ocean. *Tellus A: Dynamic Meteorology and Oceanography*, *23*(1), 28. https://doi.org/10.3402/tellusa.v23i1.10288

Huber, S. A., Balz, A., Abert, M., & Pronk, W. (2011). Characterisation of aquatic humic and non-humic matter with size-exclusion chromatography – organic carbon detection – organic nitrogen detection (LC-OCD-OND). *Water Research*, *45*(2), 879-885. https://doi.org/10.1016/j.watres.2010.09.023

Irish, V. E., Elizondo, P., Chen, J., Chou, C., Charette, J., Lizotte, M., Ladino, L. A., Wilson, T. W., Gosselin, M., Murray, B. J., Polishchuk, E., Abbatt, J. P. D., Miller, L. A., & Bertram, A. K. (2017). Ice-nucleating particles in Canadian Arctic sea-surface microlayer and bulk seawater. *Atmospheric Chemistry and Physics*, *17*(17), 10583-10595. https://doi.org/10.5194/acp-17-10583-2017

Irish, V. E., Hanna, S. J., Xi, Y., Boyer, M., Polishchuk, E., Ahmed, M., Chen, J., Abbatt, J. P. D., Gosselin, M., Chang, R., Miller, L. A., & Bertram, A. K. (2019). Revisiting properties and concentrations of ice-nucleating particles in the sea surface microlayer and bulk seawater in the Canadian Arctic during summer. *Atmospheric Chemistry and Physics*, *19*(11), 7775-7787. https://doi.org/10.5194/acp-19-7775-2019

Isono, K., Komabayasi, M., & Ono, A. (1959). Volcanoes as a Source of Atmospheric Ice Nuclei. *Nature*, *183*(4657), 317-318. https://doi.org/10.1038/183317a0

Kawana, K., Taketani, F., Matsumoto, K., Tobo, Y., Iwamoto, Y., Miyakawa, T., Ito, A., & Kanaya, Y. (2024). Roles of marine biota in the formation of atmospheric bioaerosols, cloud condensation nuclei, and ice-nucleating particles over the North Pacific Ocean, Bering Sea, and Arctic Ocean. *Atmospheric Chemistry and Physics*, *24*(3), 1777-1799. https://doi.org/10.5194/acp-24-1777-2024

Knopf, D. A., Alpert, P. A., Wang, B., & Aller, J. Y. (2011). Stimulation of ice nucleation by marine diatoms. *Nature Geoscience*, *4*(2), 88-90. https://doi.org/10.1038/ngeo1037

Knopf, D. A., Charnawskas, J. C., Wang, P., Wong, B., Tomlin, J. M., Jankowski, K. A., Fraund, M., Veghte, D. P., China, S., Laskin, A., Moffet, R. C., Gilles, M. K., Aller, J. Y., Marcus, M. A., Raveh-Rubin, S., & Wang, J. (2022). Micro-spectroscopic and freezing characterization of ice-nucleating particles collected in the marine boundary layer in the eastern North Atlantic. *Atmospheric Chemistry and Physics*, *22*(8), 5377-5398. https://doi.org/10.5194/acp-22-5377-2022

Knopf, D. A., Wang, P., Wong, B., Tomlin, J. M., Veghte, D. P., Lata, N. N., China, S., Laskin, A., Moffet, R. C., Aller, J. Y., Marcus, M. A., & Wang, J. (2023). *Physicochemical characterization of free troposphere and marine boundary layer ice-nucleating particles collected by aircraft in the eastern North Atlantic*. https://doi.org/10.5194/egusphere-2023-559

https://doi.org/10.5194/egusphere-2025-3580
Preprint. Discussion started: 8 August 2025

Lin, Y., Fan, J., Li, P., Leung, L. R., DeMott, P. J., Goldberger, L., Comstock, J., Liu, Y., Jeong, J.-H., & Tomlinson, J. (2022). Modeling impacts of ice-nucleating particles from marine aerosols on mixed-phase orographic clouds during 2015 ACAPEX field campaign. *Atmospheric Chemistry and Physics*, *22*(10), 6749-6771. https://doi.org/10.5194/acp-22-6749-2022

Mahieu, L., Whitby, H., Dulaquais, G., Tilliette, C., Guigue, C., Tedetti, M., Lefevre, D., Fourrier, P., Bressac, M., Sarthou, G., Bonnet, S., Guieu, C., & Salaün, P. (2024). Iron-binding by dissolved organic matter in the Western Tropical South Pacific Ocean (GEOTRACES TONGA cruise GPpr14). *Frontiers in Marine Science*, *11*, 1304118. https://doi.org/10.3389/fmars.2024.1304118

Marie, D., Brussaard, C. P. D., Thyrhaug, R., Bratbak, G., & Vaulot, D. (1999). Enumeration of Marine Viruses in Culture and Natural Samples by Flow Cytometry. *Applied and Environmental Microbiology*, *65*(1), 45-52. https://doi.org/10.1128/AEM.65.1.45-52.1999

McCluskey, C. S., Hill, T. C. J., Humphries, R. S., Rauker, A. M., Moreau, S., Strutton, P. G., Chambers, S. D., Williams, A. G., McRobert, I., Ward, J., Keywood, M. D., Harnwell, J., Ponsonby, W., Loh, Z. M., Krummel, P. B., Protat, A., Kreidenweis, S. M., & DeMott, P. J. (2018). Observations of Ice Nucleating Particles Over Southern Ocean Waters. *Geophysical Research Letters*, *45*(21), 11,989-11,997. https://doi.org/10.1029/2018GL079981

McCluskey, C. S., Hill, T. C. J., Malfatti, F., Sultana, C. M., Lee, C., Santander, M. V., Beall, C. M., Moore, K. A., Cornwell, G. C., Collins, D. B., Prather, K. A., Jayarathne, T., Stone, E. A., Azam, F., Kreidenweis, S. M., & DeMott, P. J. (2017). A Dynamic Link between Ice Nucleating Particles Released in Nascent Sea Spray Aerosol and Oceanic Biological Activity during Two Mesocosm Experiments. *Journal of the Atmospheric Sciences*, *74*(1), 151-166. https://doi.org/10.1175/JAS-D-16-0087.1

McCluskey, C. S., Hill, T. C. J., Sultana, C. M., Laskina, O., Trueblood, J., Santander, M. V., Beall, C. M., Michaud, J. M., Kreidenweis, S. M., Prather, K. A., Grassian, V., & DeMott, P. J. (2018). A Mesocosm Double Feature : Insights into the Chemical Makeup of Marine Ice Nucleating Particles. *Journal of the Atmospheric Sciences*, *75*(7), 2405-2423. https://doi.org/10.1175/JAS-D-17-0155.1

McCluskey, C. S., Ovadnevaite, J., Rinaldi, M., Atkinson, J., Belosi, F., Ceburnis, D., Marullo, S., Hill, T. C. J., Lohmann, U., Kanji, Z. A., O'Dowd, C., Kreidenweis, S. M., & DeMott, P. J. (2018). Marine and Terrestrial Organic Ice-Nucleating Particles in Pristine Marine to Continentally Influenced Northeast Atlantic Air Masses. *Journal of Geophysical Research: Atmospheres*, *123*(11), 6196-6212. https://doi.org/10.1029/2017JD028033

McFarquhar, G. M., Bretherton, C. S., Marchand, R., Protat, A., DeMott, P. J., Alexander, S. P., Roberts, G. C., Twohy, C. H., Toohey, D., Siems, S., Huang, Y., Wood, R., Rauber, R. M., Lasher-Trapp, S., Jensen, J., Stith, J. L., Mace, J., Um, J., Järvinen, E., … McDonald, A. (2021). Observations of Clouds, Aerosols, Precipitation, and Surface Radiation over the Southern Ocean : An Overview of CAPRICORN, MARCUS, MICRE, and SOCRATES. *Bulletin of the American Meteorological Society*, *102*(4), E894-E928. https://doi.org/10.1175/BAMS-D-20-0132.1

https://doi.org/10.5194/egusphere-2025-3580
Preprint. Discussion started: 8 August 2025

Mériguet, Z., Vilain, M., Baudena, A., Tilliette, C., Habasque, J., Lebourges-Dhaussy, A., Bhairy, N., Guieu, C., Bonnet, S., & Lombard, F. (2023). Plankton community structure in response to hydrothermal iron inputs along the Tonga-Kermadec arc. *Frontiers in Marine Science*, *10*, 1232923. https://doi.org/10.3389/fmars.2023.1232923

Mériguet, Z., Niehoff, B., Noyon, M., Panaïotis, T., Peacock, E., Picheral, M., ... & Vilain, M. (2024). *First release of the Pelagic Size Structure database: global datasets of marine size spectra obtained from plankton imaging devices. Earth Syst. Sci. Data 16, 2971–2999.*

Miyakawa, T., Taketani, F., Tobo, Y., Matsumoto, K., Yoshizue, M., Takigawa, M., & Kanaya, Y. (2023). Measurements of Aerosol Particle Size Distributions and INPs Over the Southern Ocean in the Late Austral Summer of 2017 on Board the R/V *Mirai* : Importance of the Marine Boundary Layer Structure. *Earth and Space Science*, *10*(3), e2022EA002736. https://doi.org/10.1029/2022EA002736

Moore, K. A., Hill, T. C. J., McCluskey, C. S., Twohy, C. H., Rainwater, B., Toohey, D. W., Sanchez, K. J., Kreidenweis, S. M., & DeMott, P. J. (2024). Characterizing Ice Nucleating Particles Over the Southern Ocean Using Simultaneous Aircraft and Ship Observations. *Journal of Geophysical Research: Atmospheres*, *129*(2), e2023JD039543. https://doi.org/10.1029/2023JD039543

Moutin, T., Wagener, T., Caffin, M., Fumenia, A., Gimenez, A., Baklouti, M., Bouruet-Aubertot, P., Pujo-Pay, M., Leblanc, K., Lefevre, D., Helias Nunige, S., Leblond, N., Grosso, O., & De Verneil, A. (2018). Nutrient availability and the ultimate control of the biological carbon pump in the western tropical South Pacific Ocean. *Biogeosciences*, *15*(9), 2961-2989. https://doi.org/10.5194/bg-15-2961-2018

Murray, B. J., O'Sullivan, D., Atkinson, J. D., & Webb, M. E. (2012). Ice nucleation by particles immersed in supercooled cloud droplets. *Chemical Society Reviews*, *41*(19), 6519. https://doi.org/10.1039/c2cs35200a

O'Sullivan, D., Adams, M. P., Tarn, M. D., Harrison, A. D., Vergara-Temprado, J., Porter, G. C. E., Holden, M. A., Sanchez-Marroquin, A., Carotenuto, F., Whale, T. F., McQuaid, J. B., Walshaw, R., Hedges, D. H. P., Burke, I. T., Cui, Z., & Murray, B. J. (2018). Contributions of biogenic material to the atmospheric ice-nucleating particle population in North Western Europe. *Scientific Reports*, *8*(1), 13821. https://doi.org/10.1038/s41598-018-31981-7

Porter, G. C. E., Adams, M. P., Brooks, I. M., Ickes, L., Karlsson, L., Leck, C., Salter, M. E., Schmale, J., Siegel, K., Sikora, S. N. F., Tarn, M. D., Vüllers, J., Wernli, H., Zieger, P., Zinke, J., & Murray, B. J. (2022). Highly Active Ice-Nucleating Particles at the Summer North Pole. *Journal of Geophysical Research: Atmospheres*, *127*(6), e2021JD036059. https://doi.org/10.1029/2021JD036059

Pummer, B. G., Budke, C., Augustin-Bauditz, S., Niedermeier, D., Felgitsch, L., Kampf, C. J., ... & Fröhlich-Nowoisky, J. (2015). Ice nucleation by water-soluble macromolecules. *Atmospheric Chemistry and Physics*, *15*(8), 4077-4091.

Raatikainen, T., Prank, M., Ahola, J., Kokkola, H., Tonttila, J., & Romakkaniemi, S. (2021). *The effect of marine ice nucleating particles on mixed-phase clouds*. https://doi.org/10.5194/acp-2021-537

Ralf, G., & Repeta, D. J. (1992). The pigments of Prochlorococcus marinus : The presence of divinylchlorophyll a and b in a marine procaryote. *Limnology and Oceanography*, *37*(2), 425-433. https://doi.org/10.4319/lo.1992.37.2.0425

https://doi.org/10.5194/egusphere-2025-3580
Preprint. Discussion started: 8 August 2025

Ras, J., Claustre, H., & Uitz, J. (2008). *Spatial variability of phytoplankton pigment distributions in the Subtropical South Pacific Ocean : Comparison between in situ and predicted data*. 17.

Russell, L. M., Hawkins, L. N., Frossard, A. A., Quinn, P. K., & Bates, T. S. (2010). Carbohydrate-like composition of submicron atmospheric particles and their production from ocean bubble bursting. *Proceedings of the National Academy of Sciences*, *107*(15), 6652-6657. https://doi.org/10.1073/pnas.0908905107

Schmitt-Kopplin, P., Liger-Belair, G., Koch, B. P., Flerus, R., Kattner, G., Harir, M., Kanawati, B., Lucio, M., Tziotis, D., Hertkorn, N., & Gebefügi, I. (2012). Dissolved organic matter in sea spray : A transfer study from marine surface water to aerosols. *Biogeosciences*, *9*(4), 1571-1582. https://doi.org/10.5194/bg-9-1571-2012

Schulte, T., Johanning, S., & Hofmann, E. (2010). Structure and function of native and refolded peridinin-chlorophyll-proteins from dinoflagellates. *European Journal of Cell Biology*, *89*(12), 990-997. https://doi.org/10.1016/j.ejcb.2010.08.004

Schwier, A. N., Rose, C., Asmi, E., Ebling, A. M., Landing, W. M., Marro, S., Pedrotti, M.-L., Sallon, A., Iuculano, F., Agusti, S., Tsiola, A., Pitta, P., Louis, J., Guieu, C., Gazeau, F., & Sellegri, K. (2015). Primary marine aerosol emissions from the Mediterranean Sea during pre-bloom and oligotrophic conditions : Correlations to seawater chlorophyll *a* from a mesocosm study. *Atmospheric Chemistry and Physics*, *15*(14), 7961-7976. https://doi.org/10.5194/acp-15-7961-2015

Seifert, P., Ansmann, A., Groß, S., Freudenthaler, V., Heinold, B., Hiebsch, A., Mattis, I., Schmidt, J., Schnell, F., Tesche, M., Wandinger, U., & Wiegner, M. (2011). Ice formation in ash-influenced clouds after the eruption of the Eyjafjallajökull volcano in April 2010. *Journal of Geophysical Research*, *116*, D00U04. https://doi.org/10.1029/2011JD015702

Sellegri, K., Yoon, Y. J., Jennings, S. G., O'Dowd, C. D., Pirjola, L., Cautenet, S., Chen, H., & Hoffmann, T. (2005). Quantification of Coastal New Ultra-Fine Particles Formation from *In situ* and Chamber Measurements during the BIOFLUX Campaign. *Environmental Chemistry*, *2*(4), 260. https://doi.org/10.1071/EN05074

Sinha, R. P., & Häder, D.-P. (2008). UV-protectants in cyanobacteria. *Plant Science*, *174*(3), 278-289. https://doi.org/10.1016/j.plantsci.2007.12.004

Stopelli, E., Conen, F., Zimmermann, L., Alewell, C., & Morris, C. E. (2014). Freezing nucleation apparatus puts new slant on study of biological ice nucleators in precipitation. *Atmospheric Measurement Techniques*, *7*(1), 129-134. https://doi.org/10.5194/amt-7-129-2014

Thompson, A. W., Nyerges, G., Lamberson, K. M., & Sutherland, K. R. (2024). Ubiquitous filter feeders shape open ocean microbial community structure and function. *PNAS Nexus*, *3*(3), pgae091. https://doi.org/10.1093/pnasnexus/pgae091

Thornton, D. C. O., Brooks, S. D., Wilbourn, E. K., Mirrielees, J., Alsante, A. N., Gold-Bouchot, G., Whitesell, A., & McFadden, K. (2023). Production of ice-nucleating particles (INPs) by fast-growing phytoplankton. *Atmospheric Chemistry and Physics*, *23*(19), 12707-12729. https://doi.org/10.5194/acp-23-12707-2023

Trueblood, J. V., Nicosia, A., Engel, A., Zäncker, B., Rinaldi, M., Freney, E., Thyssen, M., Obernosterer, I., Dinasquet, J., Belosi, F., Tovar-Sánchez, A., Rodriguez-Romero, A., Santachiara, G., Guieu, C., & Sellegri, K. (2021). A two-component parameterization of marine ice-nucleating particles based on seawater biology and sea spray aerosol measurements in the Mediterranean Sea. *Atmospheric Chemistry and Physics*, *21*(6), 4659-4676. https://doi.org/10.5194/acp-21-4659-2021

https://doi.org/10.5194/egusphere-2025-3580
Preprint. Discussion started: 8 August 2025

Vergara-Temprado, J., Murray, B. J., Wilson, T. W., O'Sullivan, D., Browse, J., Pringle, K. J., Ardon-Dryer, K., Bertram, A. K., Burrows, S. M., Ceburnis, D., DeMott, P. J., Mason, R. H., O'Dowd, C. D., Rinaldi, M., & Carslaw, K. S. (2017). Contribution of feldspar and marine organic aerosols to global ice nucleating particle concentrations. *Atmospheric Chemistry and Physics*, *17*(5), 3637-3658. https://doi.org/10.5194/acp-17-3637-2017

Welti, A., Bigg, E. K., DeMott, P. J., Gong, X., Hartmann, M., Harvey, M., Henning, S., Herenz, P., Hill, T. C. J., Hornblow, B., Leck, C., Löffler, M., McCluskey, C. S., Rauker, A. M., Schmale, J., Tatzelt, C., van Pinxteren, M., & Stratmann, F. (2020). Ship-based measurements of ice nuclei concentrations over the Arctic, Atlantic, Pacific and Southern oceans. *Atmospheric Chemistry and Physics*, *20*(23), 15191-15206. https://doi.org/10.5194/acp-20-15191-2020

Wilbourn, E. K., Lacher, L., Guerrero, C., Vepuri, H. S. K., Höhler, K., Nadolny, J., Pantoya, A. D., Möhler, O., & Hiranuma, N. (2024). Measurement report : A comparison of ground-level ice-nucleating-particle abundance and aerosol properties during autumn at contrasting marine and terrestrial locations. *Atmospheric Chemistry and Physics*, *24*(9), 5433-5456. https://doi.org/10.5194/acp-24-5433-2024

Wilson, T. W., Ladino, L. A., Alpert, P. A., Breckels, M. N., Brooks, I. M., Browse, J., Burrows, S. M., Carslaw, K. S., Huffman, J. A., Judd, C., Kilthau, W. P., Mason, R. H., McFiggans, G., Miller, L. A., Nájera, J. J., Polishchuk, E., Rae, S., Schiller, C. L., Si, M., … Murray, B. J. (2015). A marine biogenic source of atmospheric ice-nucleating particles. *Nature*, *525*(7568), 234-238. https://doi.org/10.1038/nature14986

Wolf, M. J., Coe, A., Dove, L. A., Zawadowicz, M. A., Dooley, K., Biller, S. J., Zhang, Y., Chisholm, S. W., & Cziczo, D. J. (2019). Investigating the Heterogeneous Ice Nucleation of Sea Spray Aerosols Using *Prochlorococcus* as a Model Source of Marine Organic Matter. *Environmental Science & Technology*, *53*(3), 1139-1149. https://doi.org/10.1021/acs.est.8b05150

Wolf, M. J., Goodell, M., Dong, E., Dove, L. A., Zhang, C., Franco, L. J., Shen, C., Rutkowski, E. G., Narducci, D. N., Mullen, S., Babbin, A. R., & Cziczo, D. J. (2020). A link between the ice nucleation activity and the biogeochemistry of seawater. *Atmospheric Chemistry and Physics*, *20*(23), 15341-15356. https://doi.org/10.5194/acp-20-15341-2020

Zobrist, B., Marcolli, C., Peter, T., & Koop, T. (2008). Heterogeneous Ice Nucleation in Aqueous Solutions : The Role of Water Activity. *The Journal of Physical Chemistry A*, *112*(17), 3965-3975. https://doi.org/10.1021/jp7112208